AD-A142 773

(12)

INVESTIGATION OF PARAMETERS INFLUENCING THE DEFLECTION OF A THICK WALL JET BY A THIN WALL JET COFLOWING OVER A ROUNDED CORNER

by
Gregory G. Huson

APPROVED FOR PUBLIC RELEASE: DISTRIBUTION UNLIMITED

AVIATION AND SURFACE EFFECTS DEPARTMENT

DTNSRDC/ASED-83/10

December 1983

DAVID W. TAYLOR NAVAL SHIP RESEARCH AND DEVELOPMENT CENTER
BETHESDA, MARYLAND 20084

DTIC FILE COPY

Best Available Copy

DTIC ELECTE JUL 1 0 1984 S E D

84 07 03 004

UNCLASSIFIED

SECURITY CLASSIFICATION OF THIS PAGE (When Date Entered)

REPORT DOCUMENTATION PAGE	READ INSTRUCTIONS BEFORE COMPLETING FORM
1. REPORT NUMBER DTNSRDC/ASED-83/10	2. GOVT ACCESSION NO. AD-A142703
	3. RECIPIENT'S CATALOG NUMBER
4. TITLE (and Subtitle) INVESTIGATION OF PARAMETERS INFLUENCING THE DEFLECTION OF A THICK WALL JET BY A THIN WALL JET COFLOWING OVER A ROUNDED CORNER	5. TYPE OF REPORT & PERIOD COVERED Final Report January 81 - July 82
	6. PERFORMING ORG. REPORT NUMBER
7. AUTHOR(s) Gregory G. Huson	8. CONTRACT OR GRANT NUMBER(s)
9. PERFORMING ORGANIZATION NAME AND ADDRESS David Taylor Naval Ship R&D Center Aviation and Surface Effects Department Bethesda, Maryland 20084	10. PROGRAM ELEMENT, PROJECT, TASK AREA & WORK UNIT NUMBERS Program Element 61152N Task Area ZR02302011 Work Unit 1660-610
11. CONTROLLING OFFICE NAME AND ADDRESS David Taylor Naval Ship R&D Center Aviation and Surface Effects Department Bethesda, Maryland 20084	12. REPORT DATE December 1983
	13. NUMBER OF PAGES 53
14. MONITORING AGENCY NAME & ADDRESS(if different from Controlling Office)	15. SECURITY CLASS. (of this report) UNCLASSIFIED
	15a. DECLASSIFICATION/DOWNGRADING SCHEDULE

16. DISTRIBUTION STATEMENT (of this Report)

APPROVED FOR PUBLIC RELEASE: DISTRIBUTION UNLIMITED

17. DISTRIBUTION STATEMENT (of the abstract entered in Block 20, if different from Report)

18. SUPPLEMENTARY NOTES

19. KEY WORDS (Continue on reverse side if necessary and identify by block number)

Circulation Control
Upper Surface Blowing
Wall Jet
Jet Deflection

20. ABSTRACT (Continue on reverse side if necessary and identify by block number)

Recent investigations proved the compatibility of the Circulation Control and the Upper Surface Blowing concepts. This static investigation is a follow-up to determine what combinations of geometric and pneumatic variables produce an effective deflection of a thick wall jet by a thin wall jet exhausting over a rounded corner. Static pressure distributions over the corner indicate that maximum deflections of the thick wall jet occur when a high average suction is distributed over the surface of the corner. Using a large corner radius, locating the source of the thick wall jet somewhat —>

DD FORM 1 JAN 73 1473 EDITION OF 1 NOV 68 IS OBSOLETE
S/N 0102-LF-014-6601

UNCLASSIFIED

SECURITY CLASSIFICATION OF THIS PAGE (When Date Entered)

Block 20 (continued)

upstream from the corner and the thin wall jet source, and using a high aspect ratio thick wall jet are geometric means of producing this type of pressure distribution.

Accession For	
NTIS GRA&I	☒
DTIC TAB	☐
Unannounced	☐
Justification	
By	
Distribution/	
Availability Codes	
Dist	Avail and/or Special
A-1	

DTIC COPY INSPECTED 2

TABLE OF CONTENTS

LIST OF FIGURES

LIST OF TABLES

NOTATION

A	Nozzle aspect ratio
h_N	Nozzle height
h_s	Coanda jet height
$\dot{m}$	Mass flow
P_s	Static pressure
P_T	Total pressure
P	Ambient pressure
R_c	Corner radius
T_o	Plenum temperature
V_j	Jet velocity
X_j	Entrainment length
θ	Jet deflection angle

ABSTRACT

Recent investigations proved the compatibility of the Circulation Control and the Upper Surface Blowing concepts. This static investigation is a follow-up to determine what combinations of geometric and pneumatic variables produce an effective deflection of a thick wall jet by a thin wall jet exhausting over a rounded corner. Static pressure distributions over the corner indicate that maximum deflections of the thick wall jet occur when a high average suction is distributed over the surface of the corner. Using a large corner radius, locating the source of the thick wall jet somewhat upstream from the corner and the thin wall jet source, and using a high aspect ratio thick wall jet are geometric means of producing this type of pressure distribution.

ADMINISTRATIVE INFORMATION

The work reported was funded by the Naval Material Command (MAT-0822) under the Independent Exploratory Development Program, Program Element 61152N, Task Area ZR0230201, and David W. Taylor Naval Ship Research and Development Center (DTNSRDC) Work Unit 1660-610.

INTRODUCTION

Recent investigations conducted at DTNSRDC have demonstrated that the jet exhaust from a turbofan engine simulator can be deflected by a thin jet sheet blowing over a rounded surface located downstream of the exhaust.[1]* These investigations were the first attempts to determine the short takeoff and landing (STOL) potential of the circulation control/upper surface blowing (CC/USB) combination.

Upper surface blowing is a flight-proven technology in which the high-velocity engine exhaust is deflected over the upper surface of an aircraft wing to achieve high lift. The advantage of this configuration is that the high-velocity exhaust jet of the engine spreads over the wing surface, thus accelerating the lower velocity air flowing over the upper wing surface and lowering its average static pressure. This increases the circulation of the wing and, consequently, the total lift.

Circulation control is also a flight-proven concept which uses a pressurized jet of air blown over the rounded trailing edge of an airfoil to increase its circulation lift.[2] The increase in lift is due to the entrainment of upstream air, which follows the rounded trailing edge contour and moves the airfoil

*A complete list of references is given on page 13.

stagnation points closer to the center of the lower surface. The change in stagnation point location effectively increases the airfoil camber.

Although earlier investigations proved the CC/USB concept viable under certain conditions,[1,3] the design of the models limited the parameter variations that influence the deflecting capability and efficiency of the CC/USB configuration. The present investigation is an attempt to establish a baseline first-order correlation of many geometric and pneumatic parameters which affect the turning efficiency and performance of a thick wall jet (upper surface blowing) exhausting over a rounded corner containing a thin wall jet or Coanda jet (circulation control).

TEST APPARATUS AND MODEL

The assembled test apparatus was designed to record thrust deflection and thus contained two strain-gage balances, as illustrated in Figures 1 and 2. One balance served as the support for the entire apparatus and measured the sum of all forces produced by the system components. The second strain-gage balance isolated the tip-turbine fans from the undercarriage. By mounting the tandem 5.5-in. tip-turbine fans to the balance, a direct measurement of the thrust produced by the thick wall jet was possible. On the exhausting side of the fans, one of three different nozzles was connected to produce rectangular thick wall jets with aspect ratios of 2, 4, or 6 (width/height); see Figures 3 and 4 and Table 1. The thick wall jet thrust deflecting model (hereafter called the thrust deflecting model) was mounted above the fan/nozzle component to deflect the thick wall jet upwards to avoid the interference effects and safety problems associated with an air jet impinging on the ground.

The thrust deflecting model consists of a plenum chamber with a circulation control blowing slot (36 in. span unless noted otherwise) through which the pressurized air of the plenum issues over a rounded corner. This model was designed to permit the use of four different radius corners for the plenum air to flow over: 0.219-, 0.438-, and 0.875-in. radius surfaces with 180 deg of arc and 0.438-in. radius surface with 96 deg of arc (Figure 4).

The thrust deflecting model was mounted on undercarriage rails with two plates serving as endplates for the model slot and plenum. The mounting of this component to the undercarriage rails enabled the entrainment length, x_j, (the distance from the thick wall jet nozzle exit plane to the slot exit location) to be

varied from 0 to 10.9 in. In addition to the variation of entrainment length and corner radius, the span of the blowing slot and corner could be changed.

The compressed air to drive the tip-turbine fans ranged to 215 psig, yielding thick wall jet thrust values up to 90 lb. Table 2 provides the conversions from thrust percentage to nominal pounds of thrust. The compressed air supplied to the plenum could also be varied, which permitted a Coanda jet momentum ($\dot{m}V_j$) range of 0 to 62 lb.

The rounded corners of the thrust deflecting model were designed with static pressure taps located at 10 to 30 deg intervals, depending on the radius of the corner. Pressure taps also were located between the thick wall jet nozzle and the blowing slot at 1-in. intervals. On the surface downstream from the rounded corners, the pressure taps were located with the same spacing and extended 6 in. forward from the corners.

The investigation was conducted in the breather tank of the transonic wind tunnel test section. This location provided access to two sources of compressed air as well as the necessary electronics to record data. In addition to the nozzle and system force measurements, temperature as well as static and total pressure measurements were recorded.

All pressure control valves and data recording equipment were located in the wind tunnel control room. This location isolated the test personnel from noise generated by the tip-turbine fans and from potential hazards of the compressed air pipes and hoses.

Because of the static nature of this investigation and the lack of a chord dimension for the thrust deflecting model, presentation of the data in the typical coefficient form was not possible. Therefore, blowing momentum coefficient was replaced with blowing momentum, $\dot{m}V_j$ (lb); rounded corner radius-to-chord ratio with corner radius, R_e (in.); and static pressure coefficient with pressure ratio, P_s/P . The momentum of the circulation control blowing jet was computed as the product of mass flow per unit span and the blowing jet velocity. Mass flow, $\dot{m}$, was measured with a venturimeter; jet velocity, V_j, was calculated using the isentropic jet velocity equation.

$$V_j = \sqrt{\frac{2\gamma RT_o}{\gamma-1}\left[1-\left(\frac{P_\infty}{P_T}\right)^{\frac{\gamma-1}{\gamma}}\right]}$$

where P_T = total plenum pressure

P_∞ = ambient pressure

T_o = plenum temperature

Thrust turning angle, θ, was computed by finding the arc tangent of the ratio of vertical-to-horizontal system forces. The efficiency of the thrust turning system was computed as the ratio of the measured total system force to the sum of the thick wall jet force and the Coanda jet blowing momentum.

DISCUSSION

WALL JET DEFLECTION PERFORMANCE

The series of curves shown in Figure 5 depict wall jet deflection, θ, as a function of Coanda jet momentum, $\dot{m}V_j$. Each plot has been generated for a constant corner radius, wall jet aspect ratio, and Coanda jet thickness. Individual curves are shown for a constant entrainment length and wall jet thrust. Table 3 is a summary of similar trends for other values of wall jet thrust. The maximum wall jet deflection angle seems most dependent on the wall jet thrust value and the corner radius. As the wall jet thrust is reduced, the maximum deflection angle increases. As the corner radius increases, the maximum deflection angle also increases. The amount of Coanda jet momentum necessary to produce these maximum deflection angles also increases with increasing corner radius, primarily because the maximum deflection angle possible is also increasing. At all wall jet thrust values other than zero, a momentum less than 25 lb is needed to achieve θ_{max} with the corner radius of 0.219 in. The 0.4375-in. corner radius requires a momentum between 25 and 40 lb to achieve θ_{max}. Coanda jet momentum values approaching 62 lb are necessary to achieve θ_{max} with the 0.875-in. corner radius. However, to attain a given wall jet deflection, more Coanda jet momentum is necessary with a small corner radius than with a large corner radius. Also, from a deflection performance standpoint, the large corner radii are better because of the larger range of deflection angles.

Two other phenomena are noted. First, at higher wall jet thrust levels and smaller corner radii, an entrainment length equal to zero produces higher deflection angles than an entrainment length greater than zero. This is contrary

to other data, which indicates that increasing entrainment length improves wall jet deflection performance. The probable cause for this phenomenon is the vectoring of the exhaust jet due to the thick wall jet nozzle design. The wall jet exhaust does not exit the nozzle parallel to the surface of the thrust turning model. Instead, the exhaust is vectored at an angle providing some "built-in" deflection when the entrainment length is zero. Figure 6 illustrates the vectoring of the wall jet by the nozzle alone. As the entrainment length is increased, the benefit of the angled wall jet decreases because the jet is directed into the surface of the thrust turning model rather than parallel to it.

The second phenomenon is illustrated in Figure 5d by the 0.438-in. radius corners. When all other conditions are the same, the corner having only 96-deg arc deflects the thick wall jet more than the corner with the full 180-deg arc. The sharp trailing edge of the 96-deg corner causes the wall jet to separate at the sharp edge resulting in wall jet deflections close to 96 deg at nearly all levels of Coanda jet momentum. The wall jet separation point of the full 180-deg arc corner moves as well as the wall jet deflection angle depending on the Coanda jet momentum level and other geometric conditions. The full arc corner, however, does have an advantage over the corner with only 96 deg of arc. When coupled with other more favorable parametric combinations, the full arc corner can produce a range of deflection angles up to 180 deg. A partial arc is limited to a smaller range of deflection angles.

DEFLECTION EFFICIENCY

The deflection efficiency is influenced most by corner radius, wall jet aspect ratio, and entrainment length. The efficiency of the wall jet thrust deflection is the ratio of resultant thrust to the sum of wall jet thrust and Coanda jet momentum. For wall jet deflection angles of less than 5 deg, the efficiency is 1.0. This implies that no thrust is lost due to small wall jet deflection; there is simply a slight change in thrust direction.

The wall jet deflection efficiency improves as the corner radius increases (Figure 7). At small deflection angles, the wall jet deflection efficiencies are nearly the same for all the corner radii; however, as the angle of deflection increases, the deflection efficiencies of the smaller corner radii decrease more rapidly.

Increasing wall jet aspect ratio improves the deflection efficiency. Results

of the aspect ratios investigated indicate that there is a diminishing incremental increase in efficiency for increasing aspect ratio. For most conditions, the difference in efficiency is very small when comparing the aspect ratio 4 and 6 wall jets, but not when comparing the aspect ratio 2 wall jet. When the entrainment length is zero, the aspect ratio 4 wall jet actually is more efficient than the aspect ratio 6 wall jet.

The deflection efficiency seems to improve with decreasing entrainment length; see Figure 7. The curves illustrate that the 0.875-in. corner radius has deflection capability limited only by the amount of Coanda jet momentum available. When these curves of various entrainment lengths are compared, the most efficient deflections occur when the entrainment length is zero. This behavior is attributed to the vectoring of the wall jet nozzle, as discussed earlier.

When the curves in Figure 7 are shifted to give the same deflection angles for no Coanda jet blowing, deflection efficiency is only slightly improved by increasing entrainment length. The smaller corner radii follow the same trends as the 0.875-in. radius; however, these radii are limited to the maximum deflection angle attainable.

STATIC PRESSURE DISTRIBUTION AT CORNER

Figure 8 shows static pressure at the smallest corner radius (0.219 in.). The flow is mostly separated over the Coanda surface. The static pressure varies near the Coanda jet slot; however, only one tap was close enough to the slot to pick up the pressure variations. The pressure variations are limited to a very small area, which means that there is no attached flow over most of the thrust turning corner. These conditions indicate that a pressure change over a very small area can significantly change the wall jet deflection angle.

The larger corner radii (0.438 and 0.875 in.) at low wall jet thrust levels (Figures 8b through 8e) show that a high suction averaged over the entire surface results in high wall jet thrust deflection angles. Less than optimum conditions can still produce large deflections of the wall jet. With an increased wall jet thrust, the amount of suction necessary to deflect the wall jet thrust is increased. Also, the suction near the Coanda jet slot is increased, and the suction on the rest of the thrust turning corner is decreased. Insufficient Coanda jet blowing or excessive blowing produces the same type of pressure distribution on

the thrust turning corner. At a very low level of $\dot{m}V_j$, not enough energy is available to develop sufficient suction; while at too high a level of $\dot{m}V_j$, there is an excess of energy to the flow over the surface which causes the wall jet to separate from the corner surface.

PRESSURE RATIO, $P_{T_{\text{Wall Jet}}}/P_{S_{\text{Slot}}}$

Maximum deflection angles under 50 deg generally occur if $X_j = 0$ and $P_{T_{\text{Wall Jet}}}/P_{S_{\text{Slot}}} < 1.95$ (Figure 9). However, corner radii of 0.438 and 0.875 in. and low wall jet thrust produce a maximum deflection angle in excess of 50 deg. The wall jet deflections are greater with larger corner radii. As the wall jet thrust increases, more suction must be maintained over the corner to obtain the same deflection angles; consequently, $P_{T_{\text{Wall Jet}}}/P_{S_{\text{Slot}}}$ must increase. As the radius of the thrust turning corner decreases, the maximum deflection angle decreases. With this decrease the pressure ratio necessary to achieve the maximum deflection increases to a point where the ratio cannot be maintained. Thus, separation of the Coanda jet from the thrust turning corner results.

PRESSURE RATIO OF JETS, $P_{T_{\text{Coanda Jet}}}/P_{T_{\text{Wall Jet}}}$

The curves for thick wall jet deflection plotted against the total pressure ratio of the Coanda jet to that of the thick wall jet fall into three groups; see Figure 10. All the curves within the 170- to 180-deg range are in the first group. This condition is the no-wall-jet-thrust case where the wall jet pressure $P_{T_{\text{Wall Jet}}}$ equals the ambient pressure. Only the Coanda jet and any ambient air near the thrust turning model are deflected, because the ambient thick wall jet is not forcing a strong suction peak at the Coanda slot or separation of the Coanda jet from the corner surface. The second group is composed of the larger corner radii with lower wall jet thrust values. These conditions produce high deflection angles (60 to 170 deg) with no definite maximum in the range of pressure ratios investigated. The third group includes the intermediate and smallest radius corners. These configurations generally reach a deflection peak at a $P_{T_{\text{Coanda Jet}}}/P_{T_{\text{Wall Jet}}}$ value of 1.7 and then smoothly decreased. Table 4 lists

the maximum wall jet deflection obtained by each corner at the maximum wall jet thrust of 100 lb.

WALL JET THICKNESS/CORNER RADIUS

The wall jet thickness/corner radius (nozzle height/corner radius) parameter is inversely proportional to turning performance, as shown in Figure 11. Each curve is divided into three sections denoting the three different corner radii. The 0.875-in. radius corner, when used in conjunction with the different aspect ratio thick wall jet nozzles, yields values of h_N/R_C less than 4. The 0.438-in. radius corner with the different nozzles yield values of h_N/R_C between 4 and 8 with the various wall jet nozzles. The 0.219-in. radius corner yields h_N/R_C values greater than 8.5. These three sections blend together smoothly enough to form a single, continuous curve at intermediate values of Coanda jet momentum. The curve shape illustrates that this parameter exerts a strong influence on the deflection performance, as do the corner radius and the wall jet thickness individually.

ASPECT RATIO

As the thick wall jet nozzle aspect ratio increases, turning performance increases (Figure 12). The sensitivity to aspect ratio change is dependent on the corner radius, as sensitivity increases with increasing corner radius. The smallest of the corner radii investigated demonstrates only a very small variation in deflection angle when compared with the larger corner radii. The larger corner radii incremental changes due to aspect ratio encompass the entire deflection angle range of the smallest corner radius. For all except the smallest corner radii, setting Coanda jet blowing at a maximum and the entrainment length greater than zero shows that the higher aspect ratio wall jets deflect more than the lower aspect ratio wall jets. This applies to the larger corner radii since the wall jet thrust deflection variation is small for the 0.219-in. corner radius.

ENTRAINMENT LENGTH

When the entrainment length, X_J, is increased while keeping other variables constant, the attainable thick wall jet deflection usually is increased (Figure 13). As the distance the thick wall jet travels from its exhaust nozzle to the Coanda jet is increased, the amount of Coanda jet momentum necessary to deflect the

thick wall jet to a specific angle decreases. This describes the behavior of the thick wall jet when either the 0.438-in. or the 0.875-in. radius corner is used. When the 0.219-in. radius corner is used, an entrainment length of zero permits the highest degree of wall jet deflection. The amount of deflection is greater with no entrainment length, because the vectoring of the wall jet by the exhaust nozzle is a significant part of the total wall jet deflection. This explanation also applies to the wall jet deflections with maximum Coanda jet blowing and a corner radius of either 0.438 in. or 0.875 in.

The sensitivity to changes in entrainment length also is influenced by the corner radius. As the corner radius increases from 0.219 to 0.875 in., the incremental increase in deflection angle generally increases as entrainment length increases. In addition, the benefit of increasing entrainment length begins to diminish at the 0.875-in. corner radius.

WALL JET/COANDA JET WIDTH INTERACTION

At each specific wall jet thrust level, an optimum thrust turning model span is combined with a Coanda jet blowing momentum which induces the maximum wall jet deflection. Increasing the thrust turning model span from this optimum will lower the deflection efficiency by providing excess Coanda jet momentum. If the span is narrower than the optimum, the maximum deflection will not occur because the span boundaries prevent the proper Coanda jet momentum to be distributed over the wall jet span (Figure 14). Optimum deflection is highly dependent on geometric variables as well as on wall jet thrust level and coanda jet momentum level. If the Coanda jet span is too wide, an apparent increase in turning is produced. The actual mechanism for this additional turning increment is the circulation control turning alone outside of the wall jet. This additional increment is due to the entrainment of ambient air. Deflecting ambient air alone with Coanda jet momentum is inefficient, as shown in Table 5.

If the span of the Coanda jet is too narrow, the Coanda jet momentum will not be able to effectively interact with the entire wall jet. Although a portion of the wall jet will be deflected, the remaining part outside the span of the Coanda jet will not be. When these conditions exist, the maximum possible wall jet deflection is less than the maximum deflection with the optimum wall jet/Coanda jet width ratio.

SUMMARY

1. The maximum wall jet deflection angle increases as corner radius increases.

2. The most influential geometric parameter is the corner radius. As the radius decreases, the influence of other geometric parameters decreases.

3. As the corner radius increases, the amount of Coanda jet momentum required to achieve maximum wall jet deflection angle increases as does the maximum value. However, a desired angle less than the maximum can be achieved with less momentum.

4. The 96-deg arc corner produces more deflection at higher wall jet thrusts with the same Coanda jet momentum than corners with the same radius and a greater arc length.

5. The wall jet deflection efficiency improves with increasing corner radius.

6. As wall jet aspect ratio increases, the wall jet deflection angle and deflection efficiency increase.

7. As the entrainment length increases, the jet deflection angle increases.

8. Decreasing entrainment length seems to improve wall jet turning efficiency.

9. As wall jet thrust increases, maximum wall jet deflection angles decreases.

10. As $P_{T_{\text{Coanda Jet}}}/P_{T_{\text{Wall Jet}}}$ increases, the wall jet deflection angle increases.

11. Increasing $P_{T_{\text{Wall Jet}}}/P_{S_{\text{Slot}}}$ increases the wall jet deflection nozzle.

12. As the span of the Coanda jet increases, wall jet deflection angles increase; however, the total efficiency decreases.

13. Highest wall jet deflection angles occur when there is a high, evenly distributed suction over the thrust turning corner.

CONCLUSIONS

Efficient deflection of a thick wall jet can be produced using a thin Coanda jet exhausting over a rounded corner. To maximize the amount the wall jet can be deflected, the radius of the corner must be large, as must be the wall jet aspect ratio and the distance between wall jet nozzle and the Coanda jet slot. The span of the Coanda slot should be approximately the "natural" span of the wall jet after it is allowed to grow and mix with the ambient air.

Static pressure ratio distributions over the surface of the corner indicate that for high deflection angles an even suction distribution over the surface is required. Given a particular design point, it should be possible to tailor the shape of the corner to provide the prescribed deflection at a minimum energy cost.

The span of the Coanda jet relative to the wall jet, or the two-dimensionality, determines the efficiency and effectiveness of the system. The optimum span ratio is one which limits the span of the Coanda jet to that of the wall jet after it travels the entrainment length mixing with ambient air. This condition ensures that the maximum amount of Coanda jet blowing will be used to deflect the wall jet without permitting excess Coanda blowing to entrain static ambient air.

ACKNOWLEDGMENTS

The author especially thanks Michael Harris for developing the data reduction program and assisting in the data collection. Acknowledgment is extended to Ronald Adams, Louis Cregger, Robert Englar, James Nichols, Jr., and Ossie Steffanelli for their assistance and interest throughout this investigation.

REPERENCES

1. Harris, M.J., "Investigation of the Circulation Control Wing/Upper Surface Blowing High-Lift System on a Low Aspect Ratio Semispan Model," DTNSRDC/ASED-81/10 (May 1981).

2. Englar, R.J. et al., "Design of the Circulation Control Wing STOL Demonstrator Aircraft," AIAA Paper No. 79-1842 presented at the AIAA Aircraft Systems and Technology Meeting, New York (20-22 Aug 1979).

3. Harris, M.J. et al., "Development of the Circulation Control Wing/Upper Surface Blowing Powered-Lift System for STOL Aircraft," ICAS Paper No. 82-6.5.1 presented at the 13th Congress of the International Council of the Aeronautical Sciences Meeting, Seattle (22-27 Aug 1982).

PRECEDING PAGE BLANK-NOT FILMED

TABLE 1 - THICK WALL JET THRUST CONVERSION

Percentage Thrust Setting	Approximate Thrust (lb)	Range (lb)
100	92	80 - 106
70	63	50 - 71
35	30	26 - 31

TABLE 2 - THICK WALL JET NOZZLE SPECIFICATIONS

A	Height (in.)	Width (in.)
2	3.3	6.5
4	2.3	9.2
6	1.9	11.3

PRECEDING PAGE BLANK-NOT FILMED

TABLE 3 - MAXIMUM WALL JET DEFLECTION FOR A SPECIFIC WALL JET THRUST AND CORNER RADIUS

Wall Jet Thrust (lb)	Corner Radius (in.)		
	0.219	0.437	0.875
0	180 deg	180 deg	179 deg
29	37	172	173
70	18	54	159
90	14	30	97

TABLE 4 - MAXIMUM WALL JET DEFLECTIONS AT MAXIMUM WALL JET THRUST

R_c (in.)	θ_{max} (deg)	$P_{T_{CJ}}/P_{T_{WJ}}$	A	X_j (in.)	h_s (in.)
0.219	14	1.35	4	0	0.028
0.437	29	1.97	4	0	0.028
0.437	29	1.65	6	10.9	0.014
0.875	140	2.23	6	10.9	0.028

TABLE 5 - WALL JET DEFLECTION FOR VARYING SLOT SPAN TO NOZZLE SPAN RATIO
(Corner radius = 0.875 in; nozzle AR = 2)

Entrainment Length / Corner Radius	Thrust Level (lb)	Wall Jet Def. Angle (deg)	Coanda Jet Momentum (lb)	Slot Span / Nozzle Span
$X_j/R = 0$	70	21	3.7	1
		27 (θ_{max})	10.2	
	90	20	3.0	2
		23 (θ_{max})	15.0	
		20	7.0	5
		28 (θ_{max})	47.0	
$X_j/R = 12.4$	70	20	3.3	1
		30 (θ_{max})	10.8	
	90	20	2.0	2
		40 (θ_{max})	15.8	
		20	7.0	5
		45 (θ_{max})	48.0	

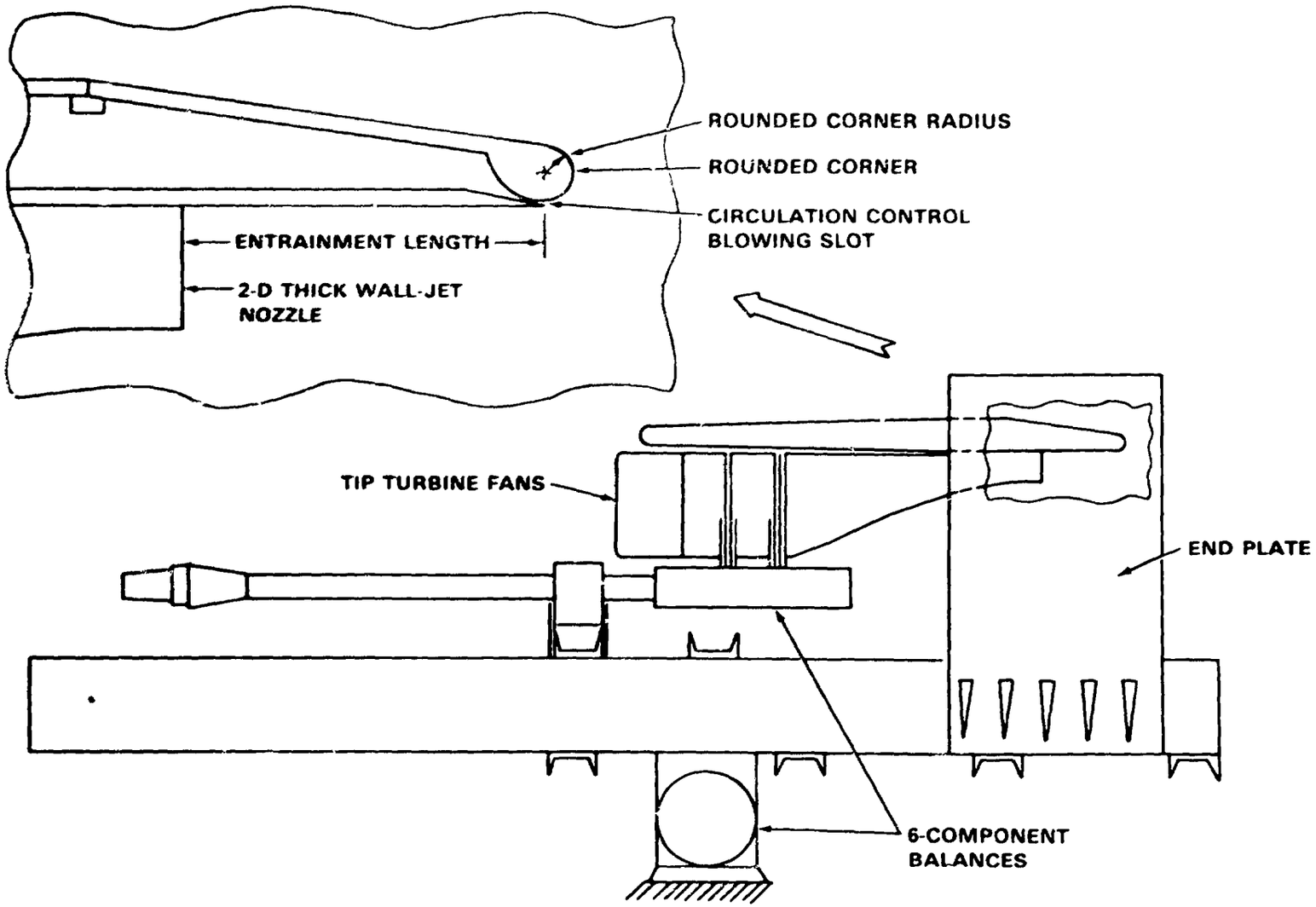

Figure 1 - Test Configuration

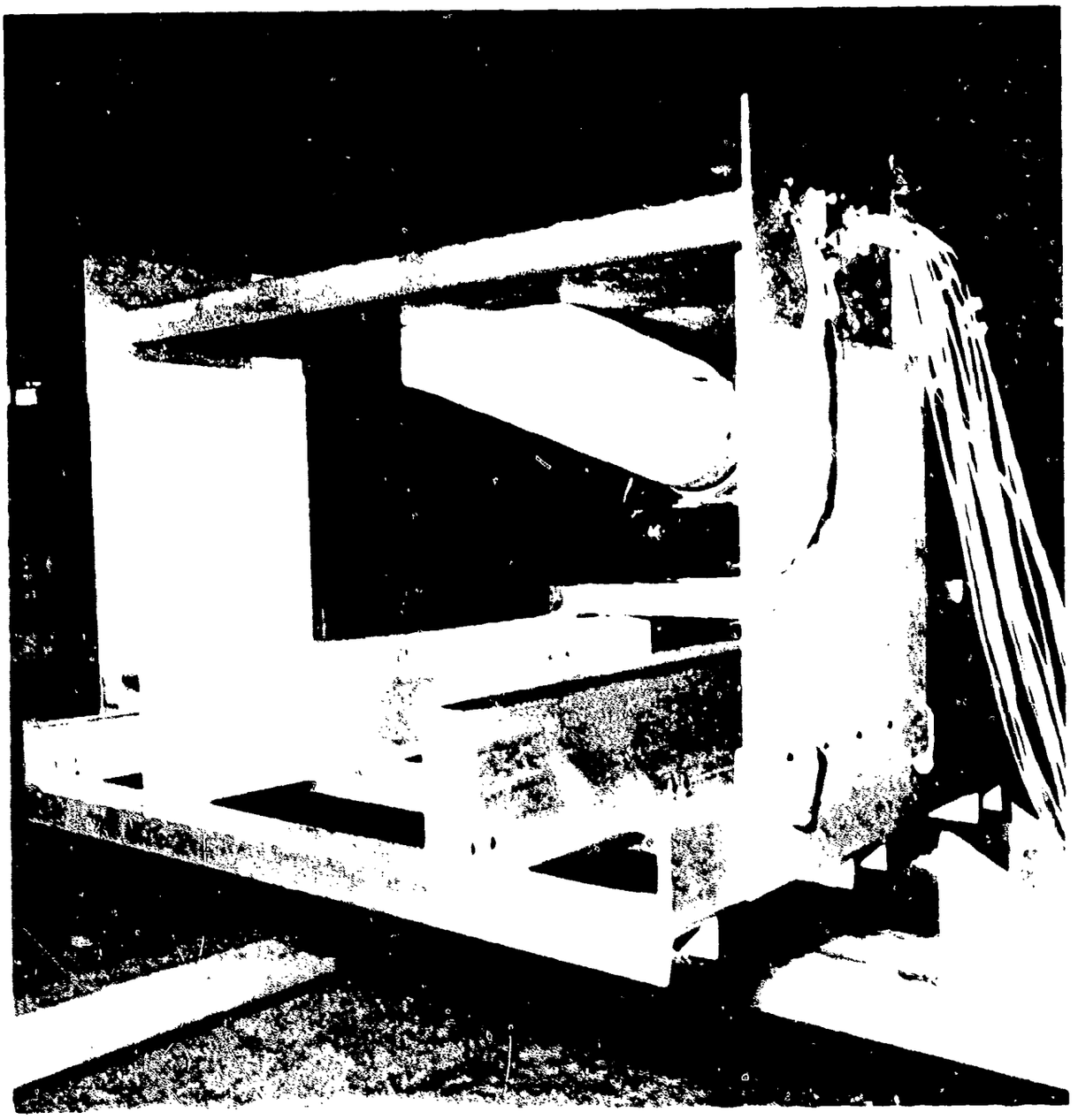

Figure 2 - Test Apparatus

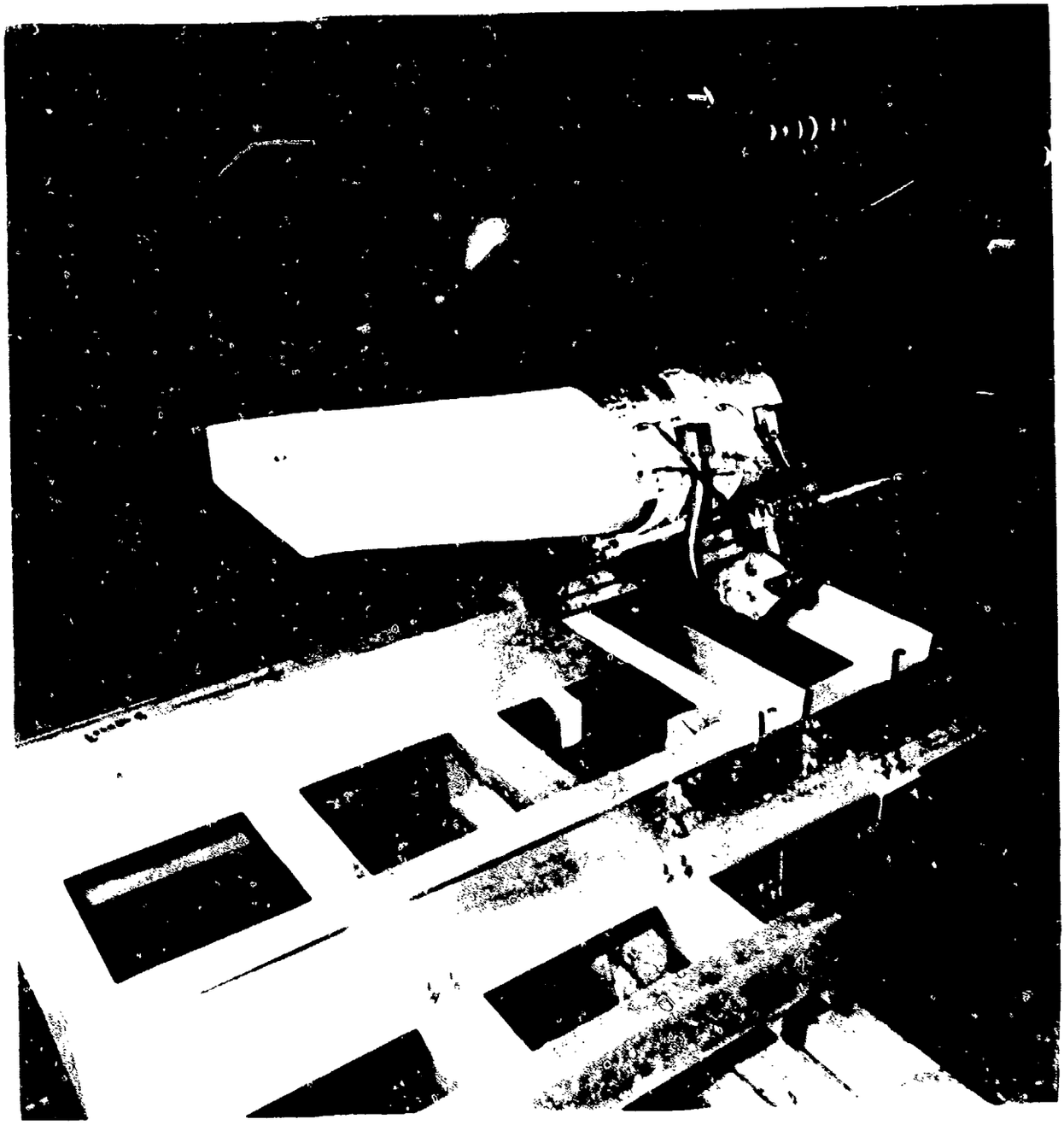

Figure 3 - Tip-Turbine Fans, AR = 4 Thick Wall Jet Nozzle, and Undercarriage

Figure 4 - Corner Radii of 0.219, 0.438, and 0.875 Inches and Thick Wall Jet Nozzles

Figure 5 - Wall Jet Deflection Performance

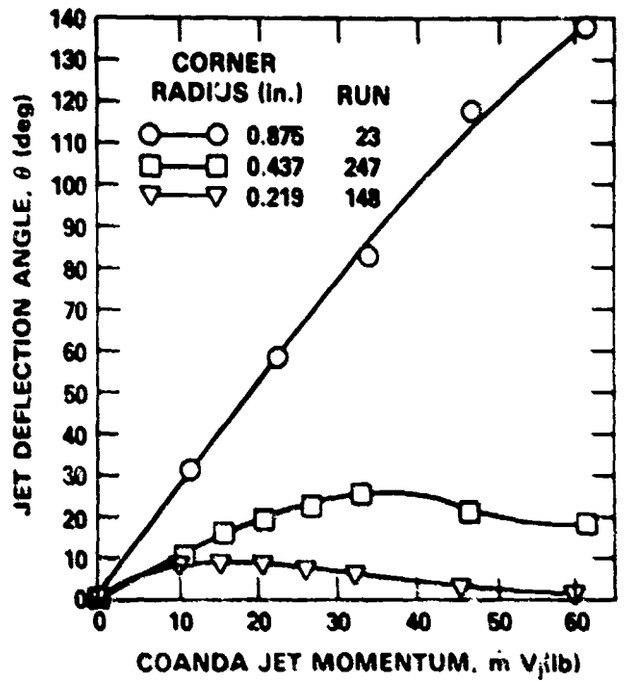

Figure 5a - Wall Jet AR = 6; Entrainment Length = 10.9 Inches; Wall Jet Thrust = 100 Percent (~90 Pounds); Coanda Jet Height = 0.028 Inches

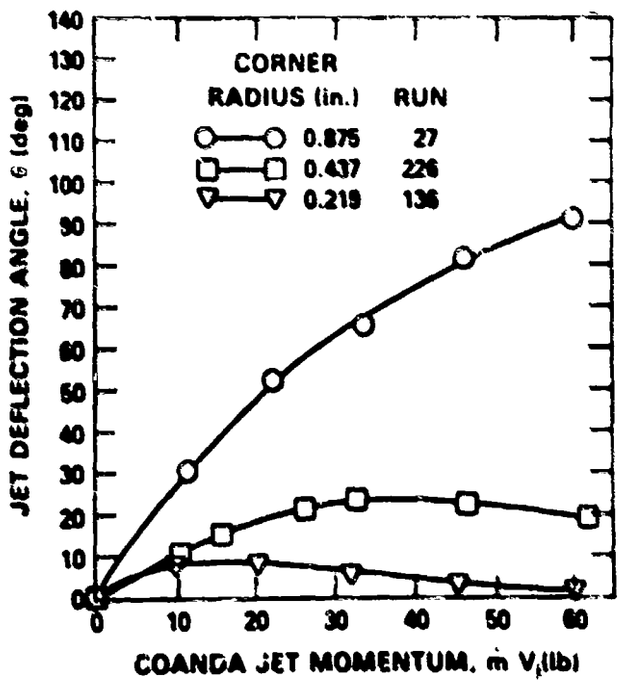

Figure 5b - Wall Jet AR = 4; Entrainment Length = 10.9 Inches; Wall Jet Thrust = 100 Percent (~90 Pounds); Coanda Jet Height = 0.028 Inches

Figure 5 (Continued)

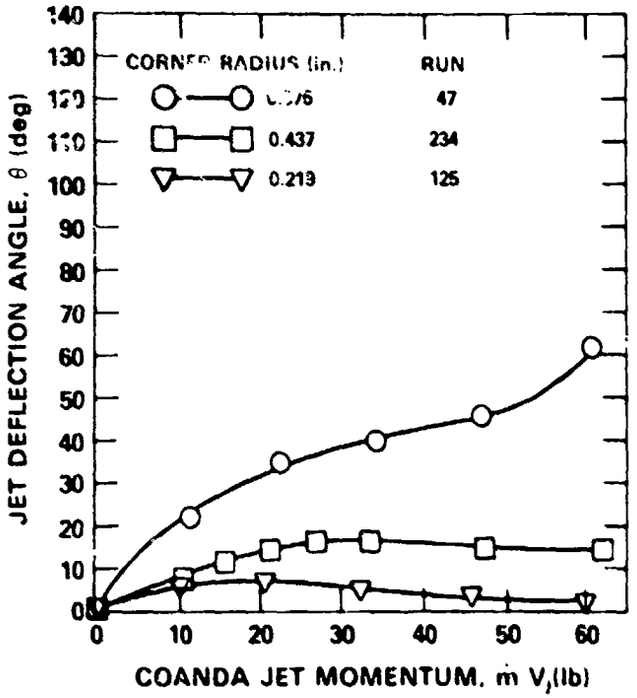

Figure 5c - Wall Jet AR = 2; Entrainment Length = 10.9 Inches; Wall Jet Thrust = 100 Percent (~90 Pounds); Coanda Jet Height = 0.028 Inches

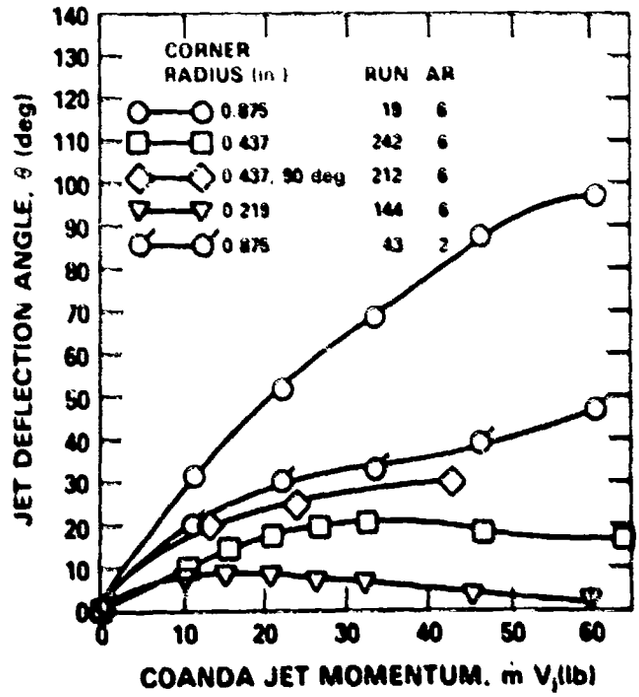

Figure 5d - Entrainment Length = 5.2 Inches; Wall Jet Thrust = 100 Percent (~90 Pounds); Coanda Jet Height = 0.028 Inches

Figure 5 (Continued)

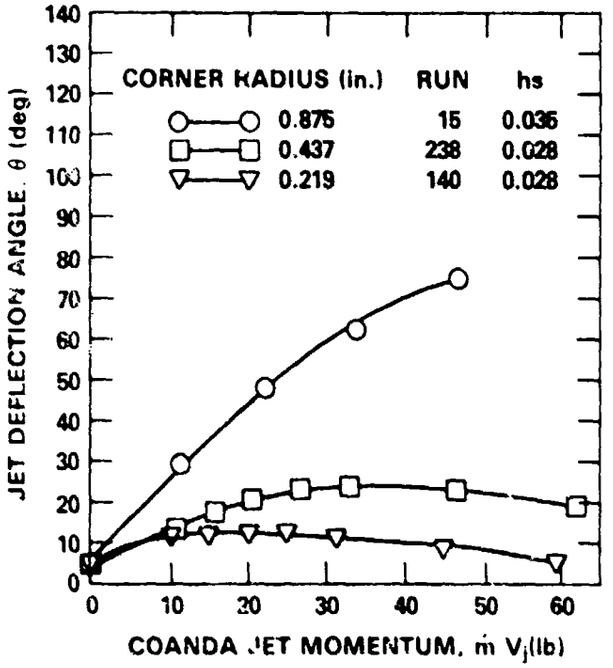

Figure 5e - Wall Jet AR = 6; Entrainment Length = 0 Inches; Wall Jet Thrust = 100 Percent (~90 Pounds); Coanda Jet Height = 0.028 Inches

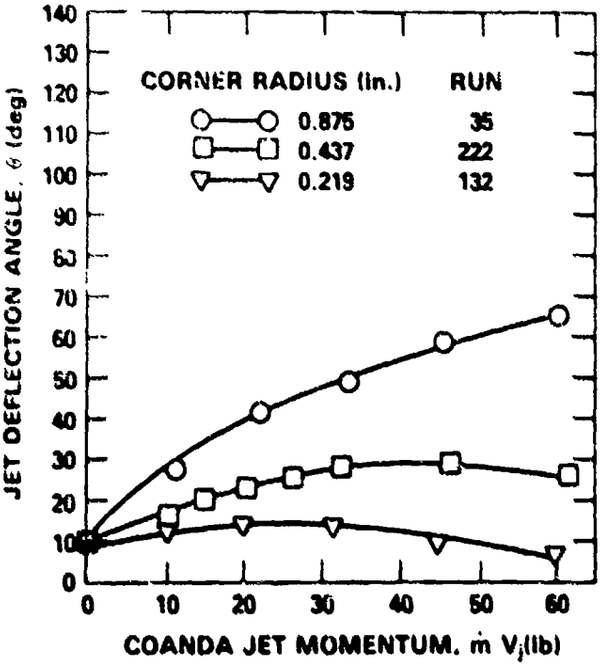

Figure 5f - Wall Jet AR = 4; Entrainment Length = 0 Inches; Wall Jet Thrust = 100 Percent (~90 Pounds); Coanda Jet Height = 0.028 Inches

Figure 5 (Continued)

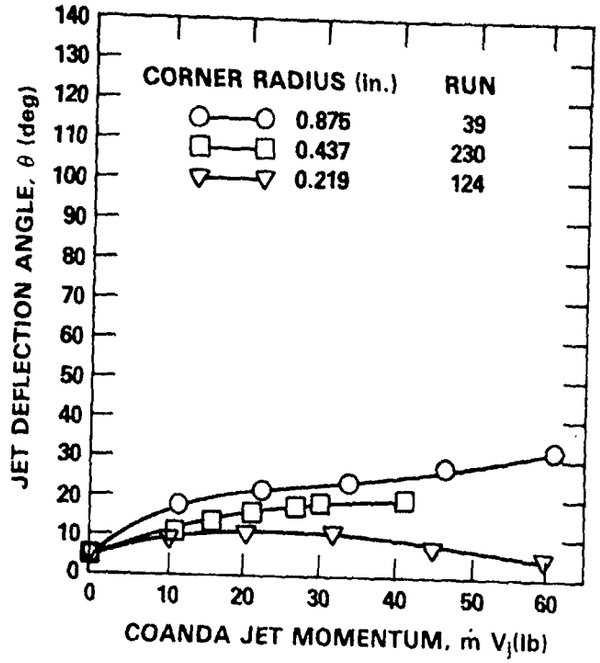

Figure 5g - Wall Jet AR = 2; Entrainment Length = 0 Inches; Wall Jet Thrust = 100 Percent (~90 Pounds); Coanda Jet Height = 0.028 Inches

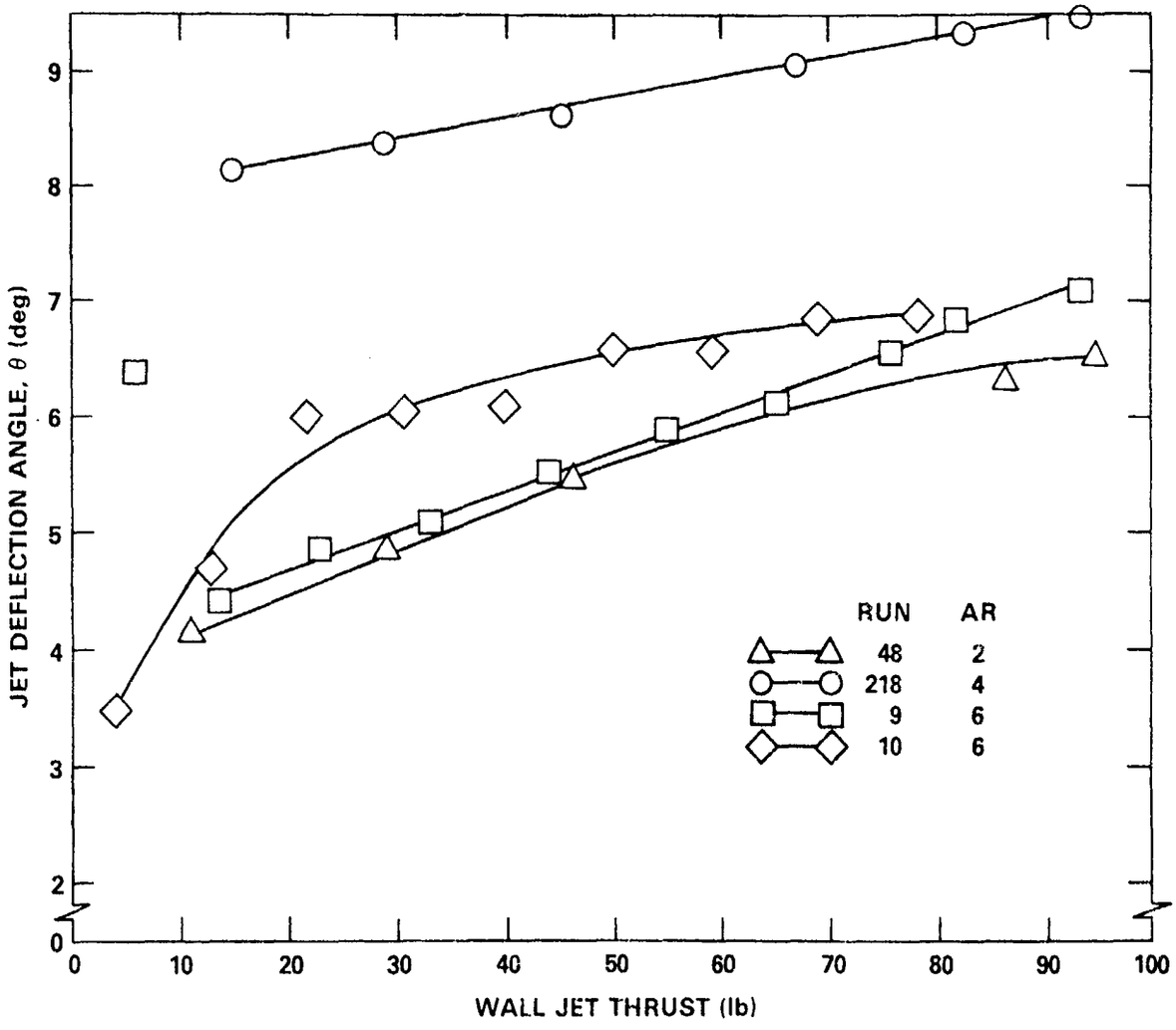

Figure 6 - Wall Jet Deflection Due to Nozzles

Figure 7 - Wall Jet Deflection Efficiency

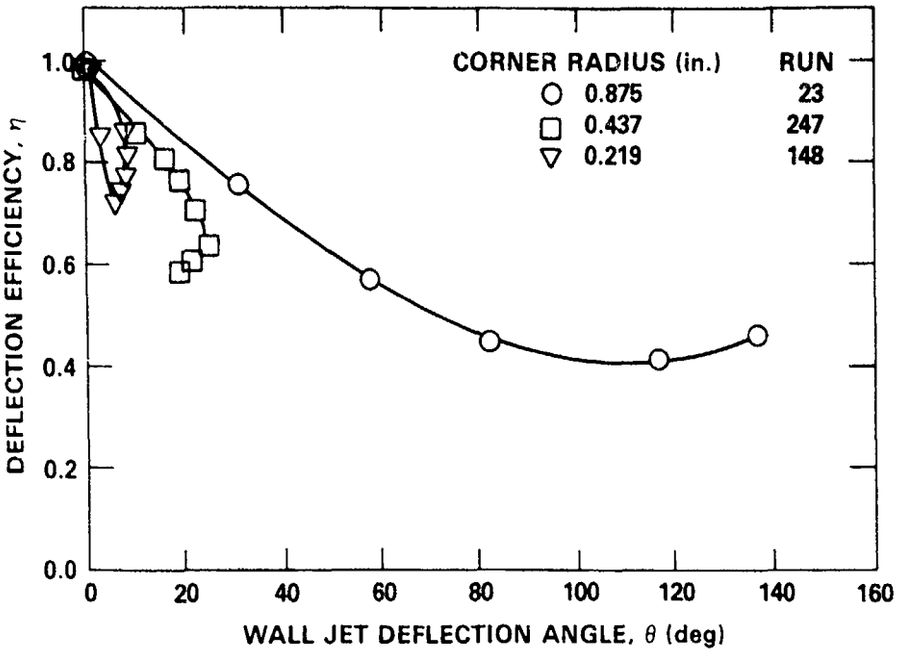

Figure 7a - Wall Jet AR = 6; Entrainment Length = 10.9 Inches; Wall Jet Thrust = 100 Percent (~90 Pounds); Coanda Jet Height = 0.028 Inches

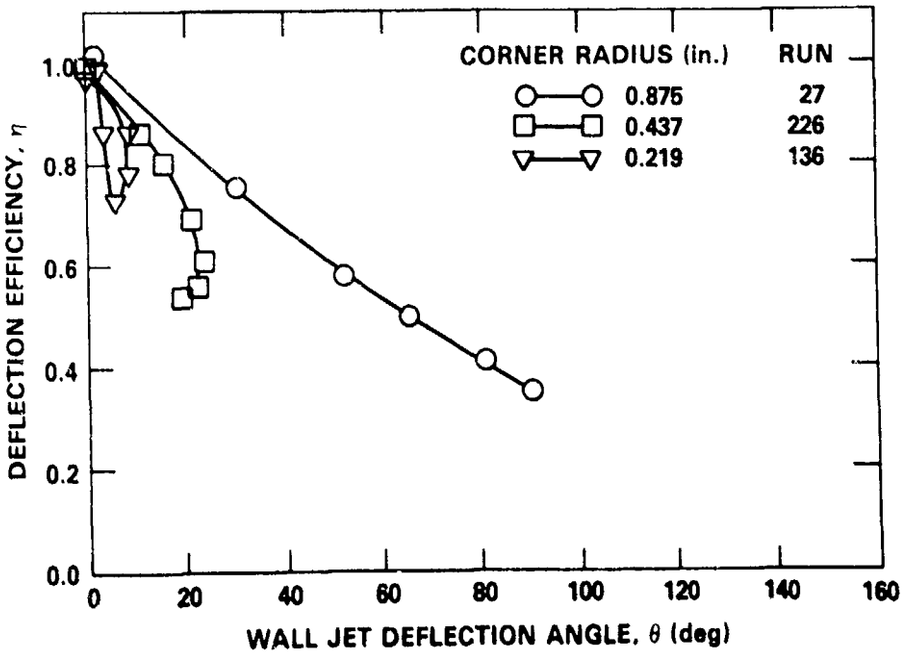

Figure 7b - Wall Jet AR = 4; Entrainment Length = 10.9 Inches; Wall Jet Thrust = 100 Percent (~90 Pounds); Coanda Jet Height = 0.028 Inches

Figure 7 (Continued)

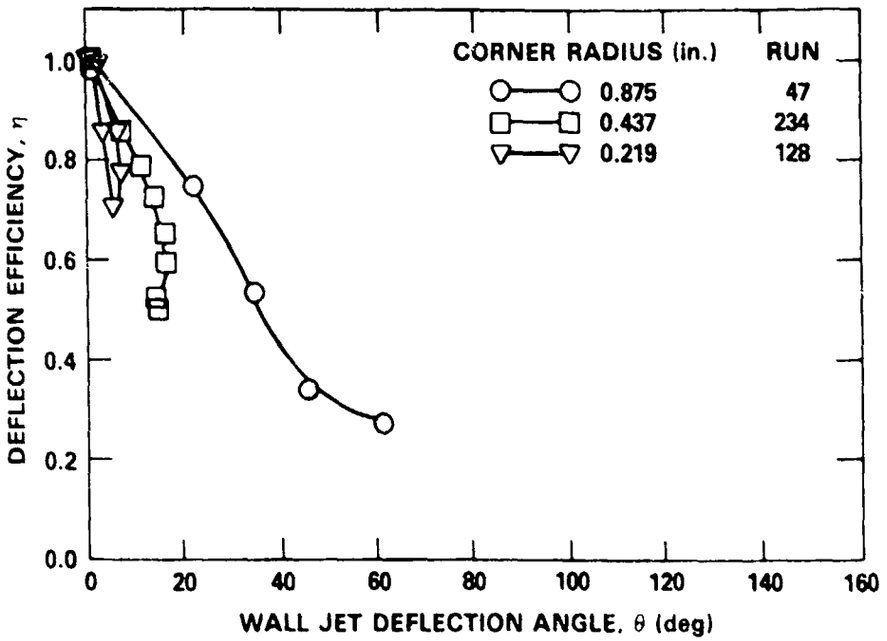

Figure 7c - Wall Jet AR = 2; Entrainment Length = 10.9 Inches; Wall Jet Thrust = 100 Percent (~90 Pounds); Coanda Jet Height = 0.028 Inches

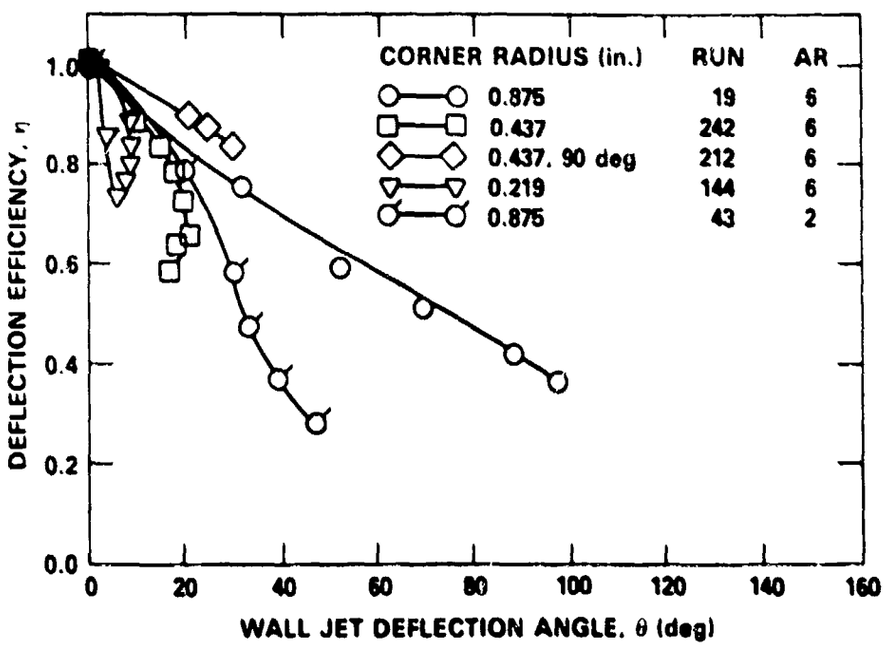

Figure 7d - Entrainment Length = 5.2 Inches; Wall Jet Thrust = 100 Percent (~90 Pounds); Coanda Jet Height = 0.028 Inches

Figure 7 (Continued)

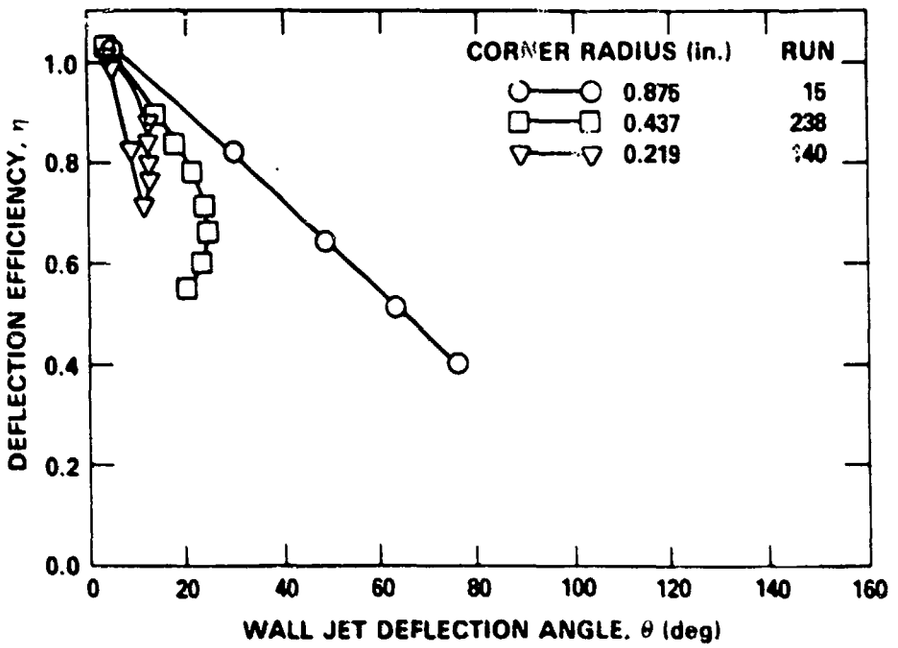

Figure 7e - Wall Jet AR = 6; Entrainment Length = 0 Inches; Wall Jet Thrust = 100 Percent (~90 Pounds); Coanda Jet Height = 0.028 Inches

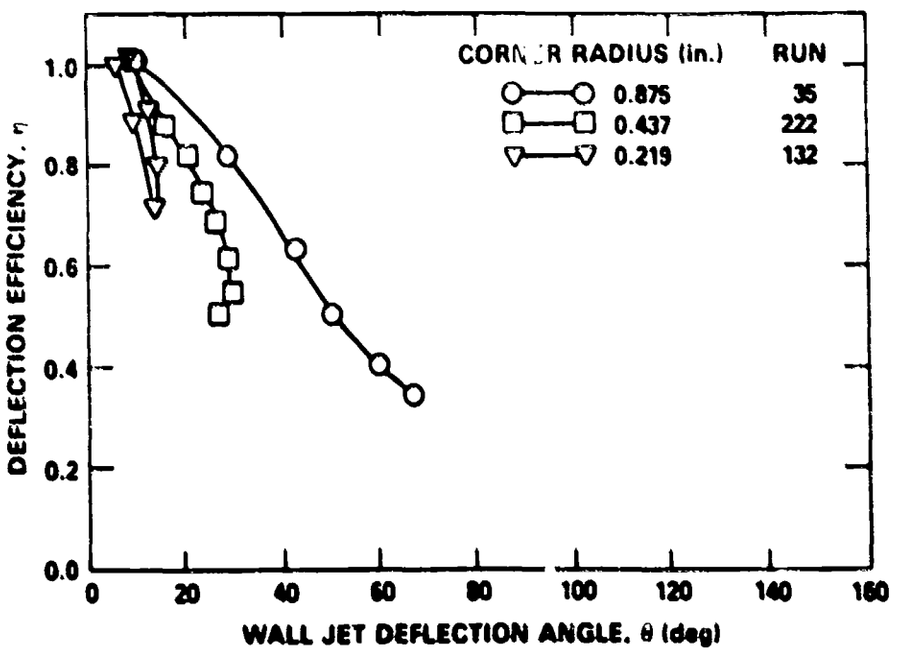

Figure 7f - Wall Jet AR = 4; Entrainment Length = 0 Inches; Wall Jet Thrust = 100 Percent (~90 Pounds); Coanda Jet Height = 0.028 Inches

Figure 7 (Continued)

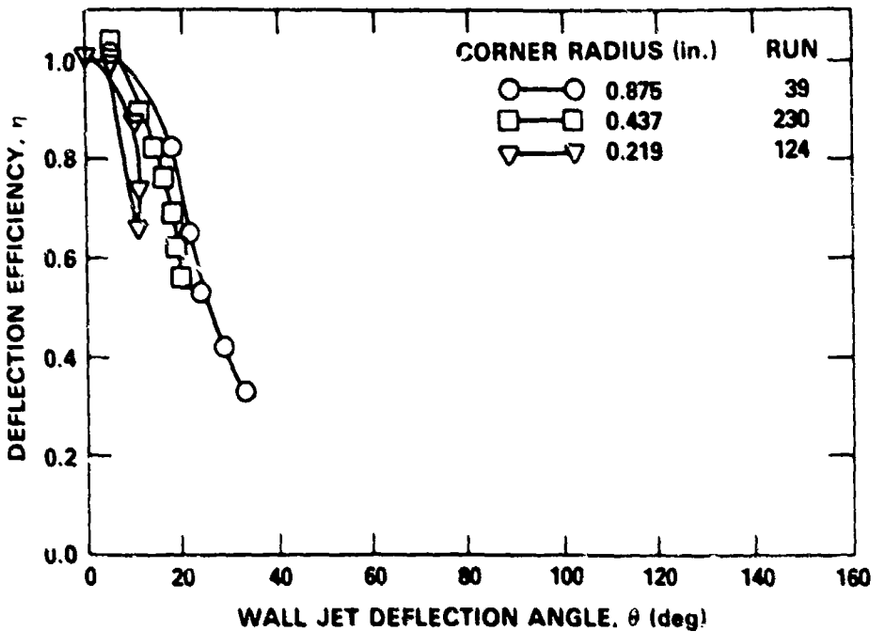

Figure 7g - Wall Jet AR = 2; Entrainment Length = 0 Inches; Wall Jet Thrust = 100 Percent (~90 Pounds); Coanda Jet Height = 0.028 Inches

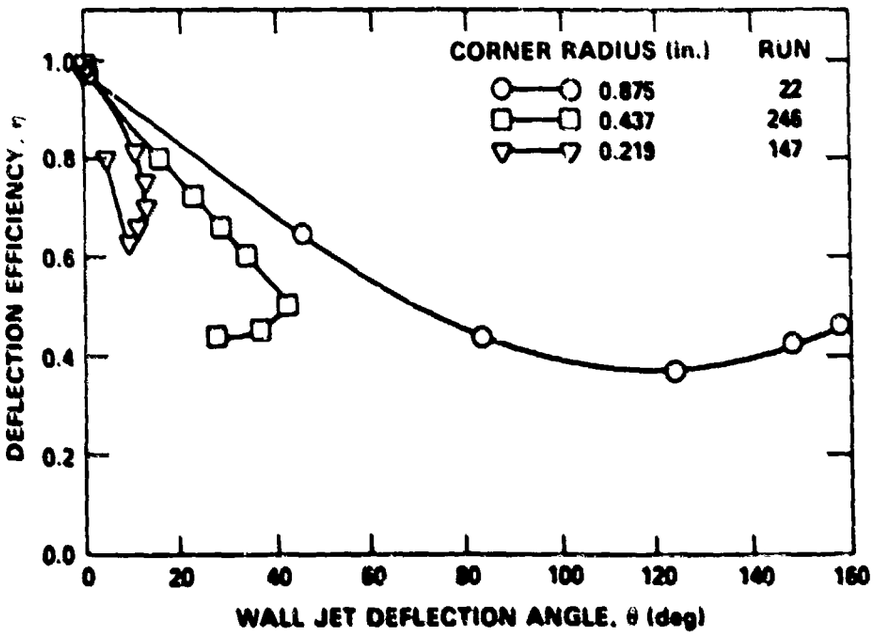

Figure 7h - Wall Jet AR = 6; Entrainment Length = 10.9 Inches; Wall Jet Thrust = 70 Percent (~70 Pounds); Coanda Jet Height = 0.028 Inche

Figure 7 (Continued)

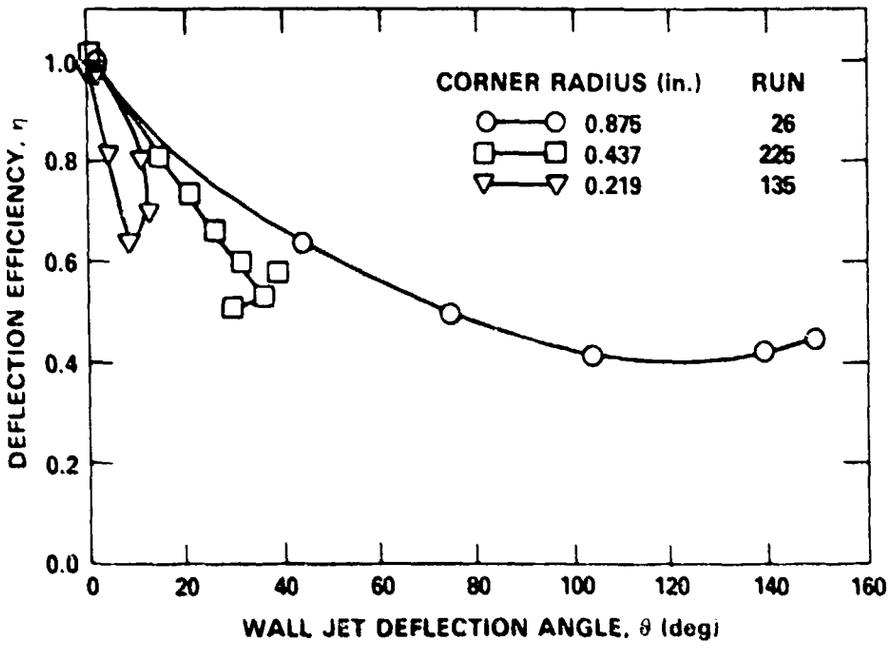

Figure 7i - Wall Jet AR = 4; Entrainment Length = 10.9 Inches; Wall Jet Thrust = 70 Percent (~70 Pounds); Coanda Jet Height = 0.028 Inches

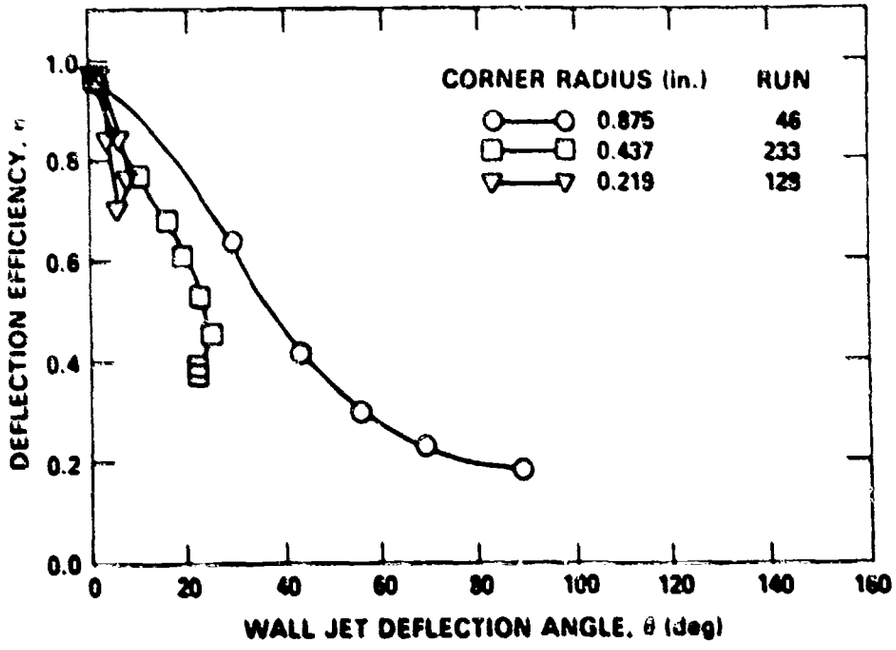

Figure 7j - Wall Jet AR = 2; Entrainment Length = 10.9 Inches; Wall Jet Thrust = 70 Percent (~70 Pounds); Coanda Jet Height = 0.028 Inches

Figure 7 (Continued)

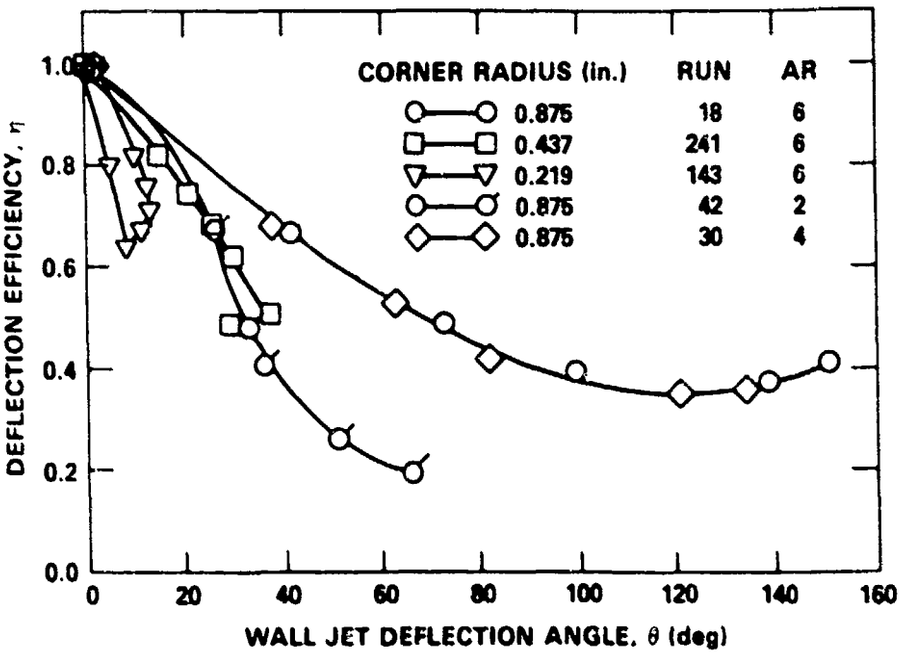

Figure 7k - Entrainment Length = 5.2 Inches; Wall Jet Thrust = 70 Percent (~70 Pounds); Coanda Jet Height = 0.028 Inches

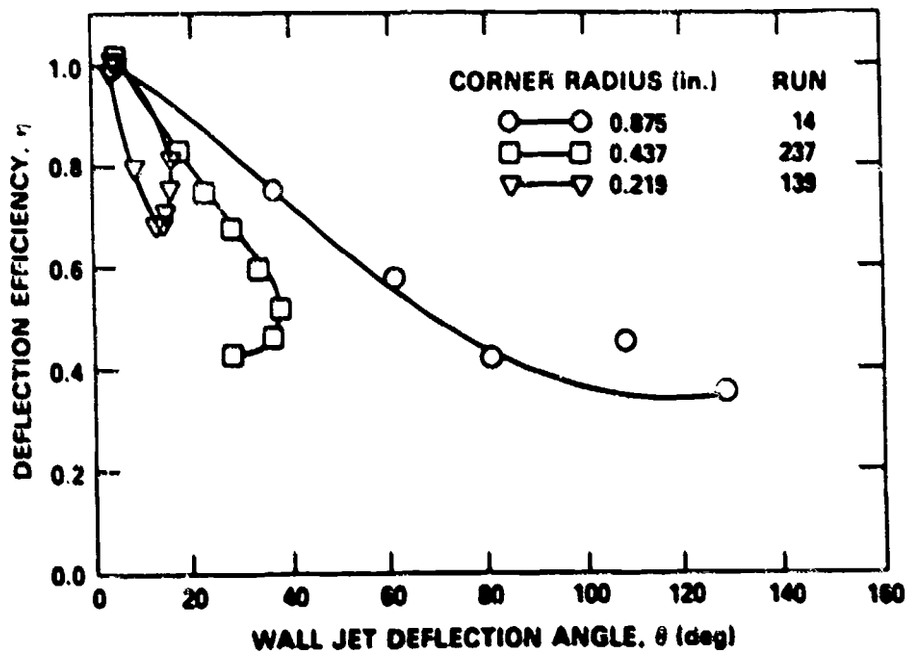

Figure 7l - Wall Jet AR = 6; Entrainment Length = 0 Inches; Wall Jet Thrust = 70 Percent (~70 Pounds); Coanda Jet Height = 0.028 Inches

Figure 7 (Continued)

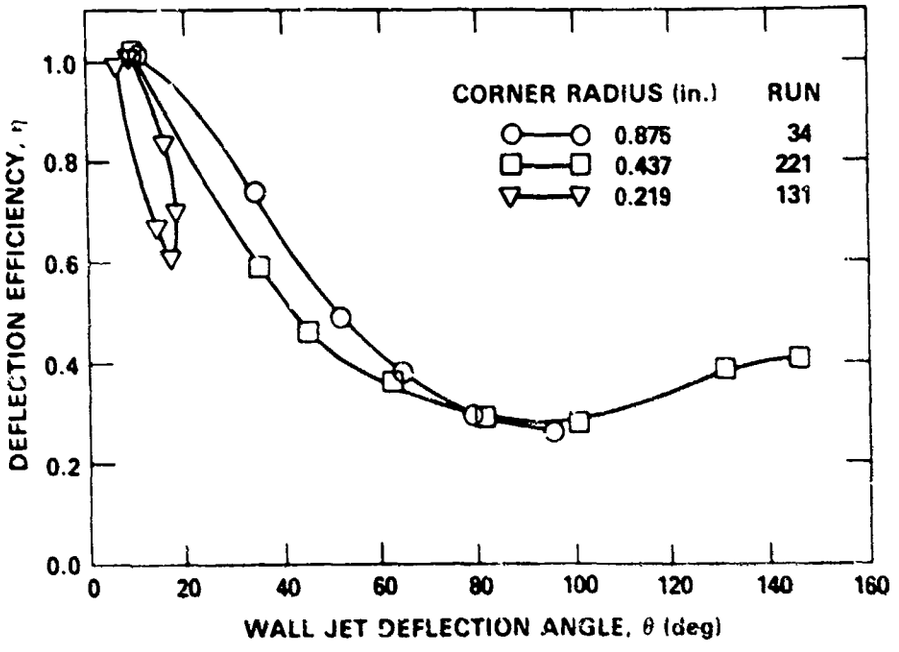

Figure 7m - Wall Jet AR = 4; Entrainment Length = 0 Inches; Wall Jet Thrust = 70 Percent (~70 Pounds); Coanda Jet Height = 0.028 Inches

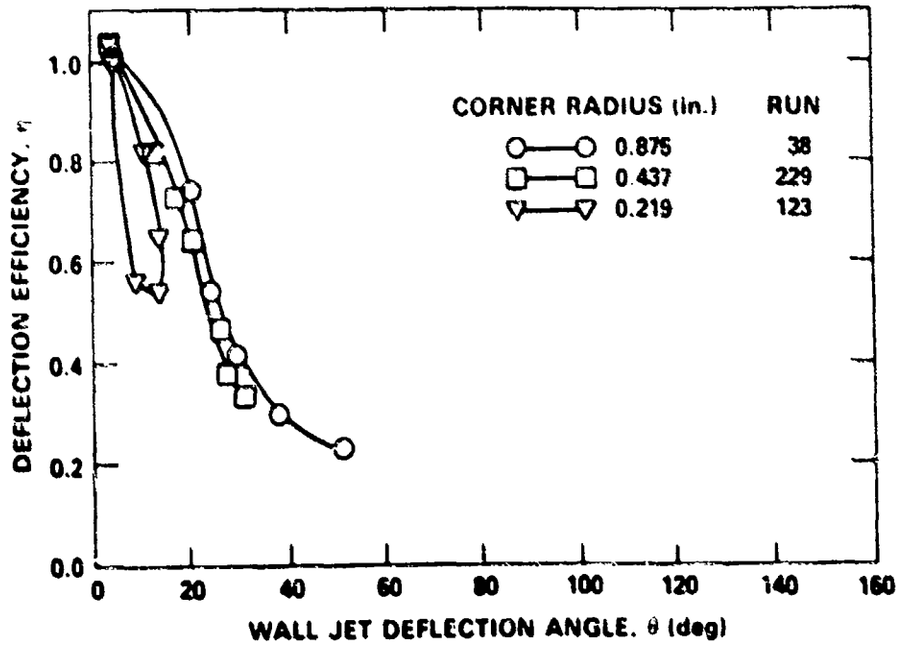

Figure 7n - Wall Jet AR = 2; Entrainment Length = 0 Inches; Wall Jet Thrust = 70 Percent (~70 Pounds), Coanda Jet Height = 0.028 Inches

Figure 8 - Static Pressure Distribution of Rounded Corner

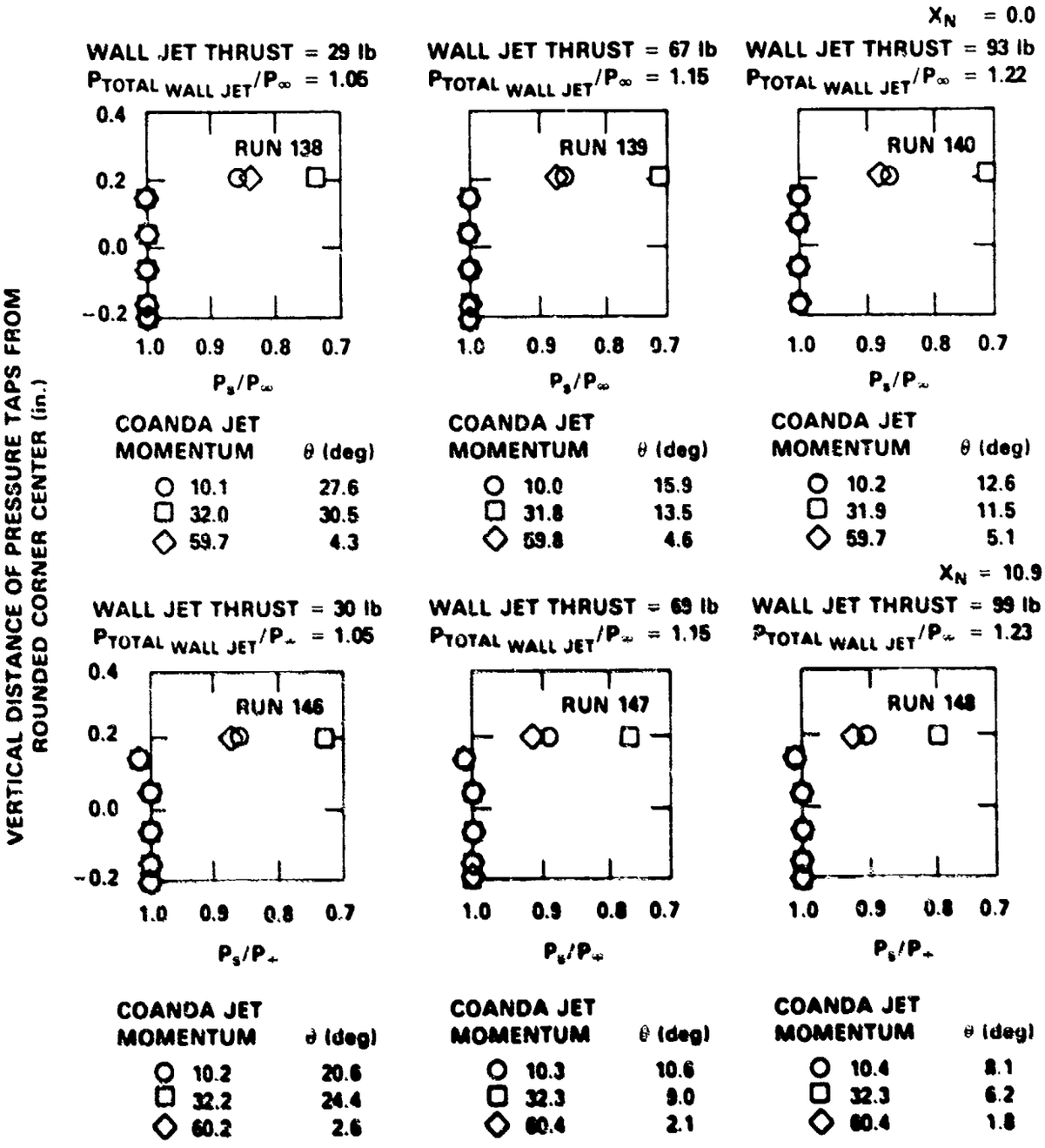

Figure 8a - Wall Jet AR = 6; Entrainment Length = 0 Inches; Corner Radius 0.219 Inches; Coanda Jet Height = 0.028 Inches

Figure 8 (Continued)

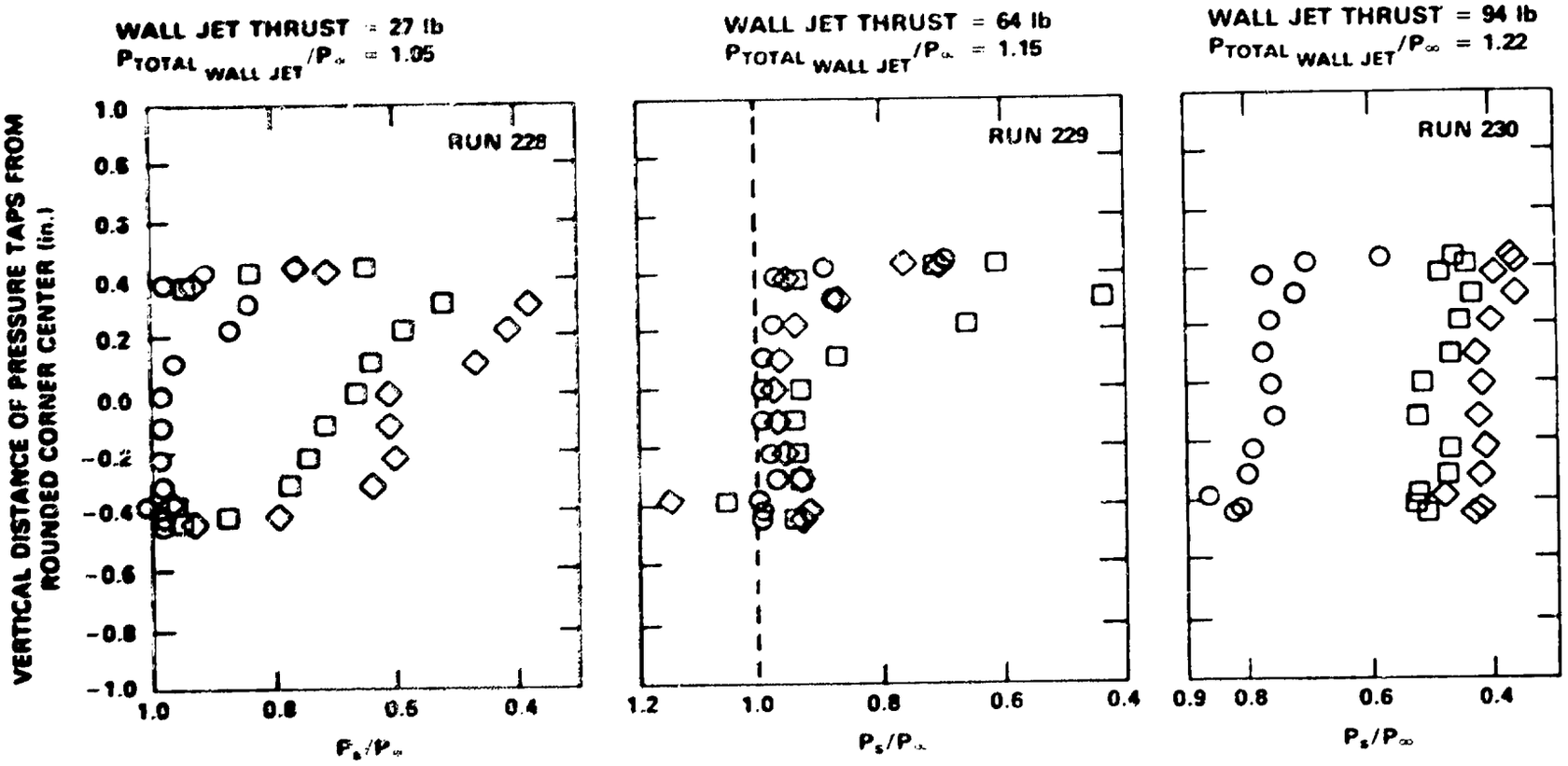

COANDA JET MOMENTUM	θ (deg)
10.6	22.1
33.2	80.4
62.7	140.7

COANDA JET MOMENTUM	θ (deg)
10.5	12.8
33.0	26.3
62.4	31.1

COANDA JET MOMENTUM	θ (deg)
10.6	10.8
33.1	18.4
62.3	19.7

Figure 8b - Wall Jet AR = 2; Entrainment Length = 0 Inches; Corner Radius = 0.4375 Inches; Coanda Jet Height = 0.028 Inches

Figure 8 (Continued)

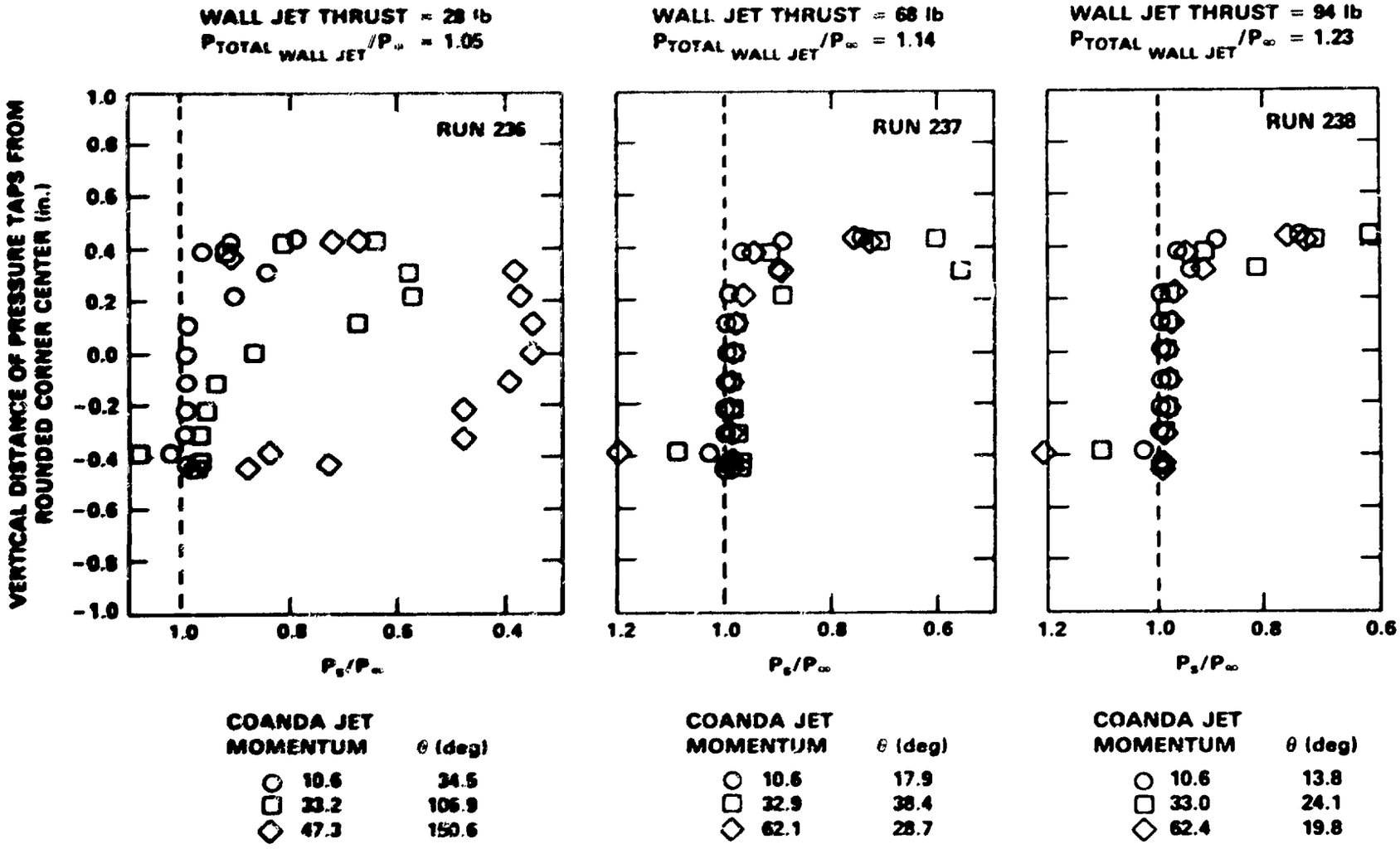

Figure 8c - Wall Jet AR = 6; Entrainment Length = 0 Inches;
Corner Radius = 0.4375 Inches; Coanda Jet Height = 0.028 Inches

Figure 8 (Continued)

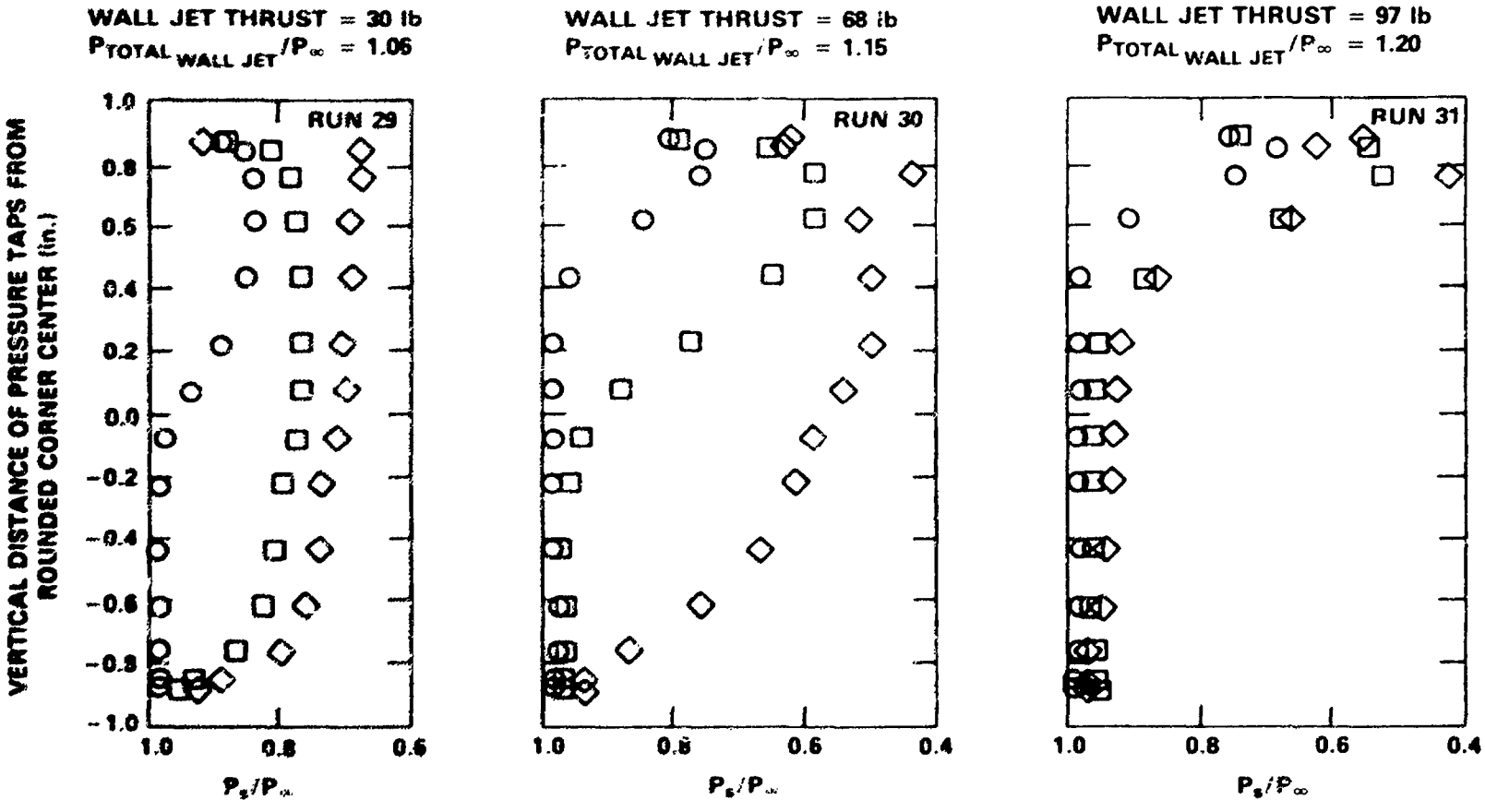

Figure 8d - Wall Jet AR = 4; Entrainment Length = 5.2 Inches; Corner Radius = 0.875 Inches; Coanda Jet Height = 0.035 Inches

Figure 8 (Continued)

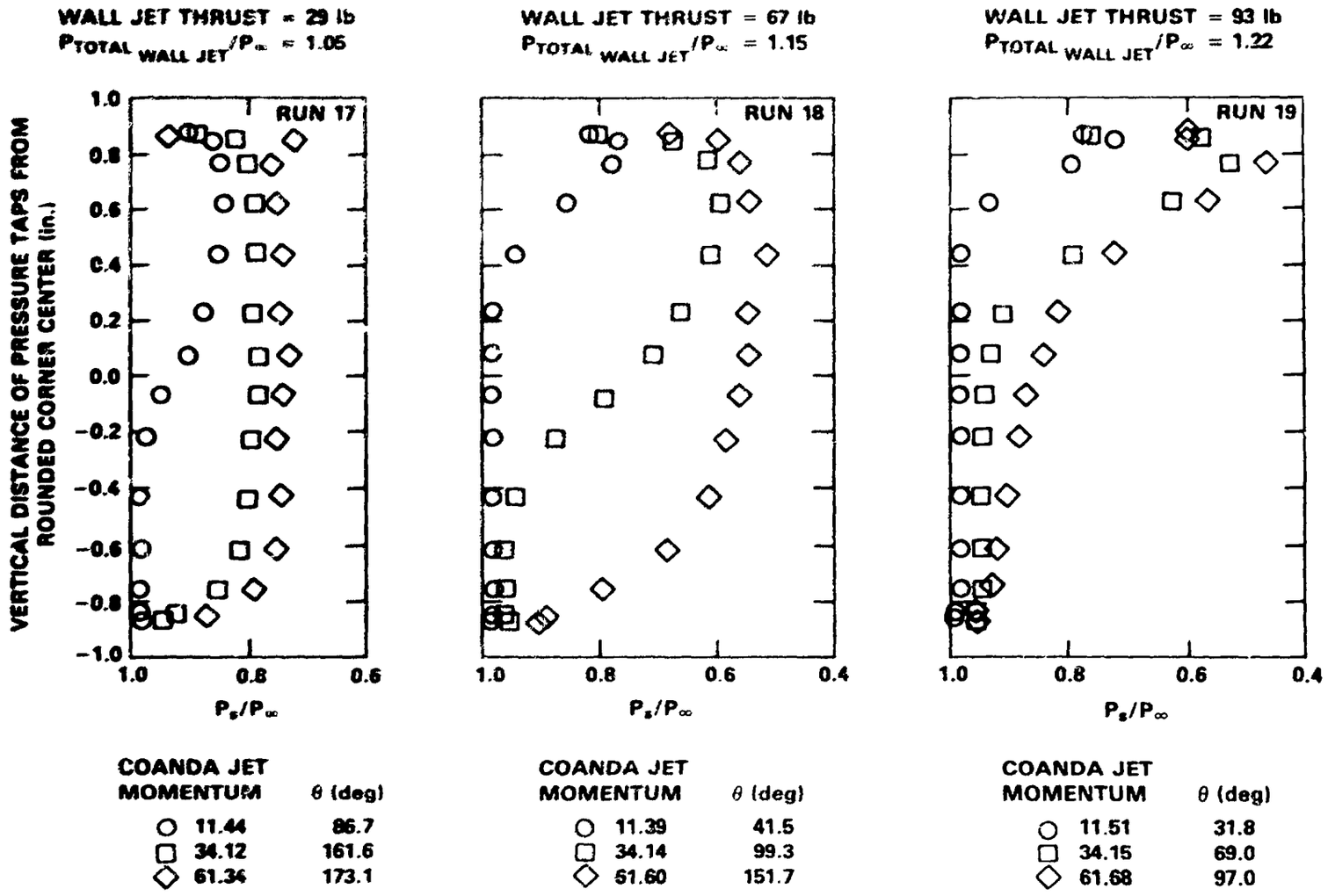

Figure 8e - Wall Jet AR = 6; Entrainment Length = 5.2 Inches; Corner Radius = 0.875 Inches; Coanda Jet Height = 0.035 Inches

Figure 9 - $P_{Total\ Wall\ Jet}/P_{Static\ Slot}$ Influence on Wall Jet Deflection Performance

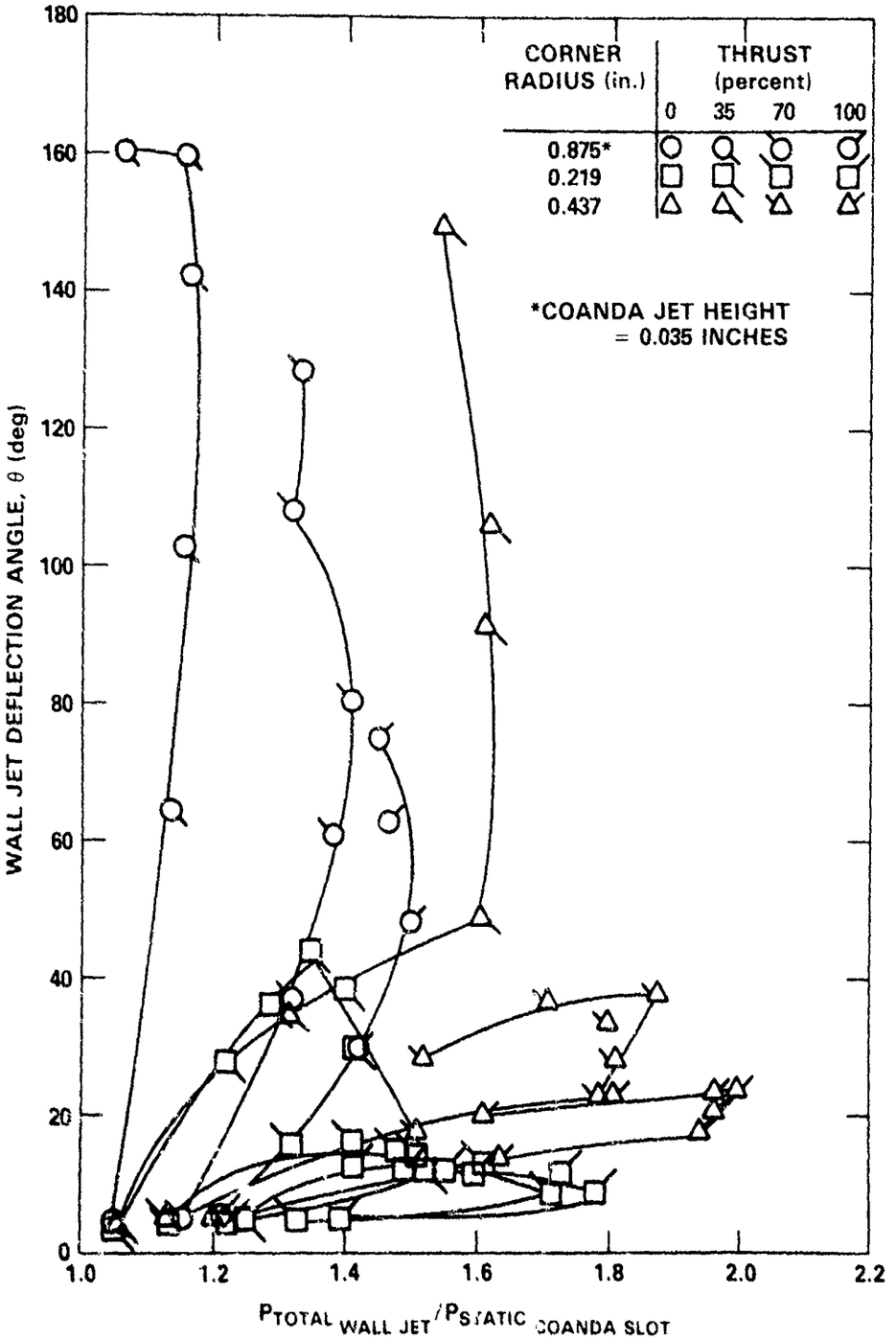

Figure 9a - Wall Jet AR = 6; Entrainment Length = 0 Inches; Coanda Jet Height = 0.028 Inches

Figure 9 (Continued)

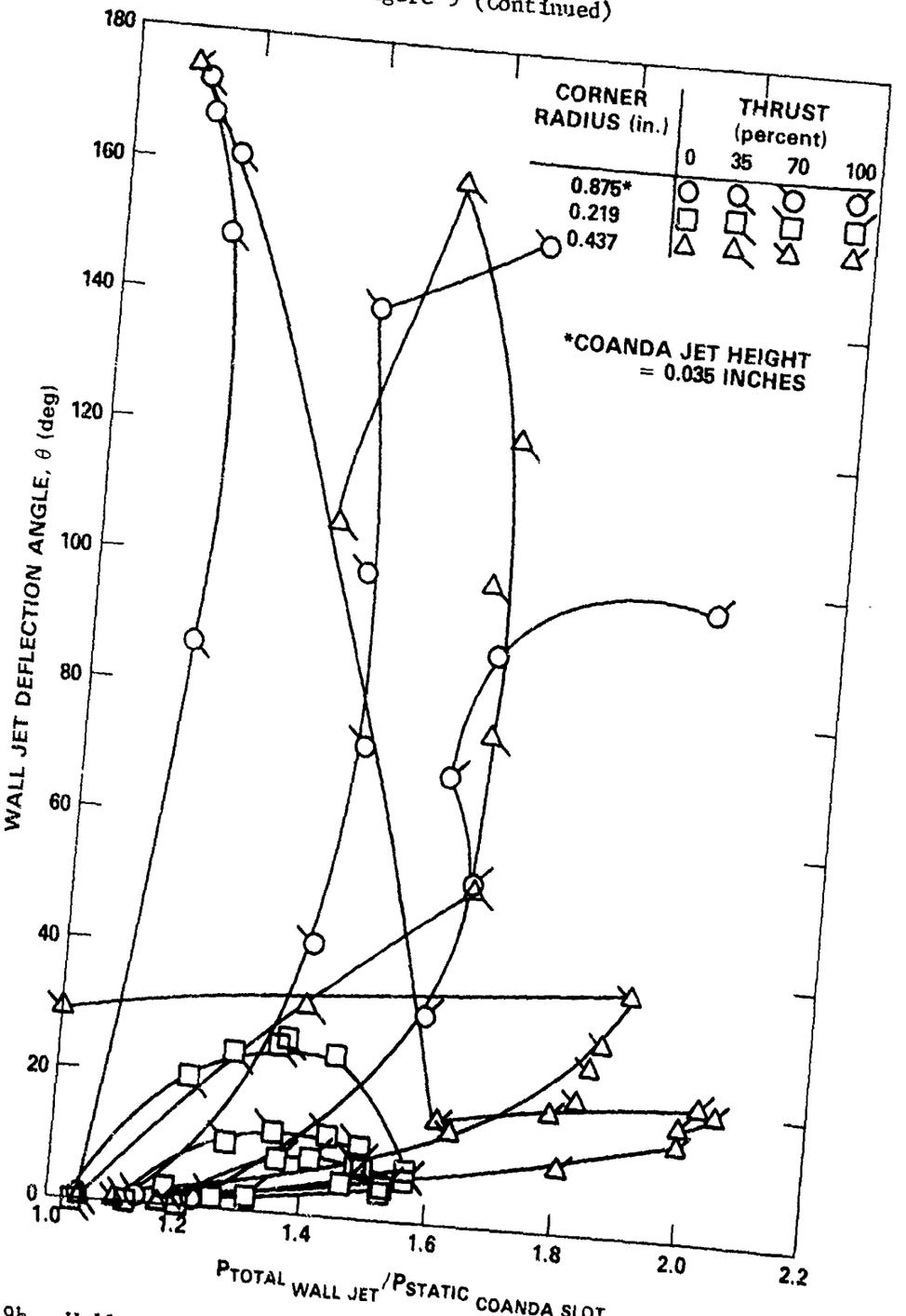

Figure 9b - Wall Jet AR = 6; Entrainment Length = 5.2 Inches; Coanda Jet Height = 0.028 Inches

Figure 9 (Continued)

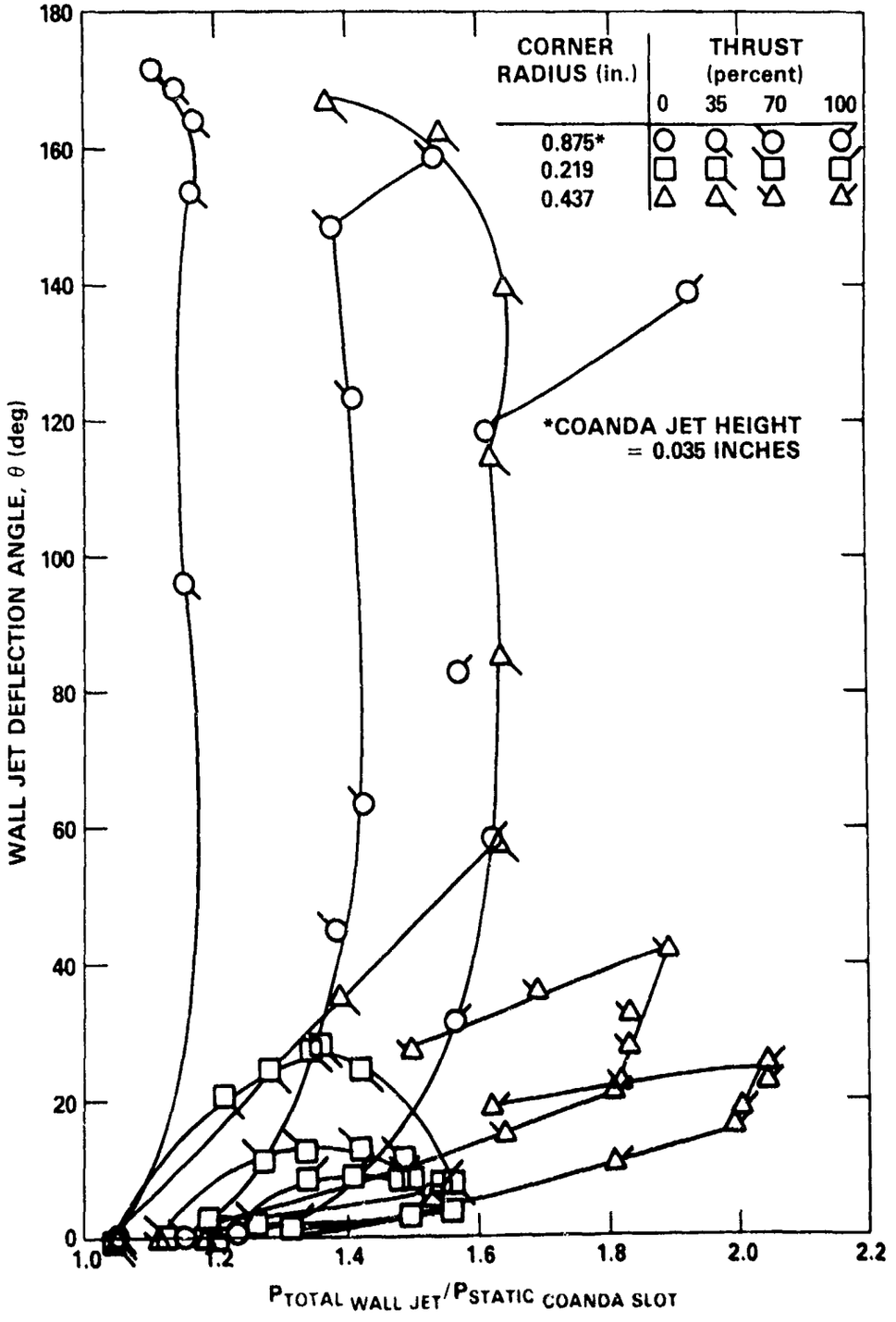

Figure 9c - Wall Jet AR = 6; Entrainment Length = 10.9 Inches; Coanda Jet Height = 0.028 Inches

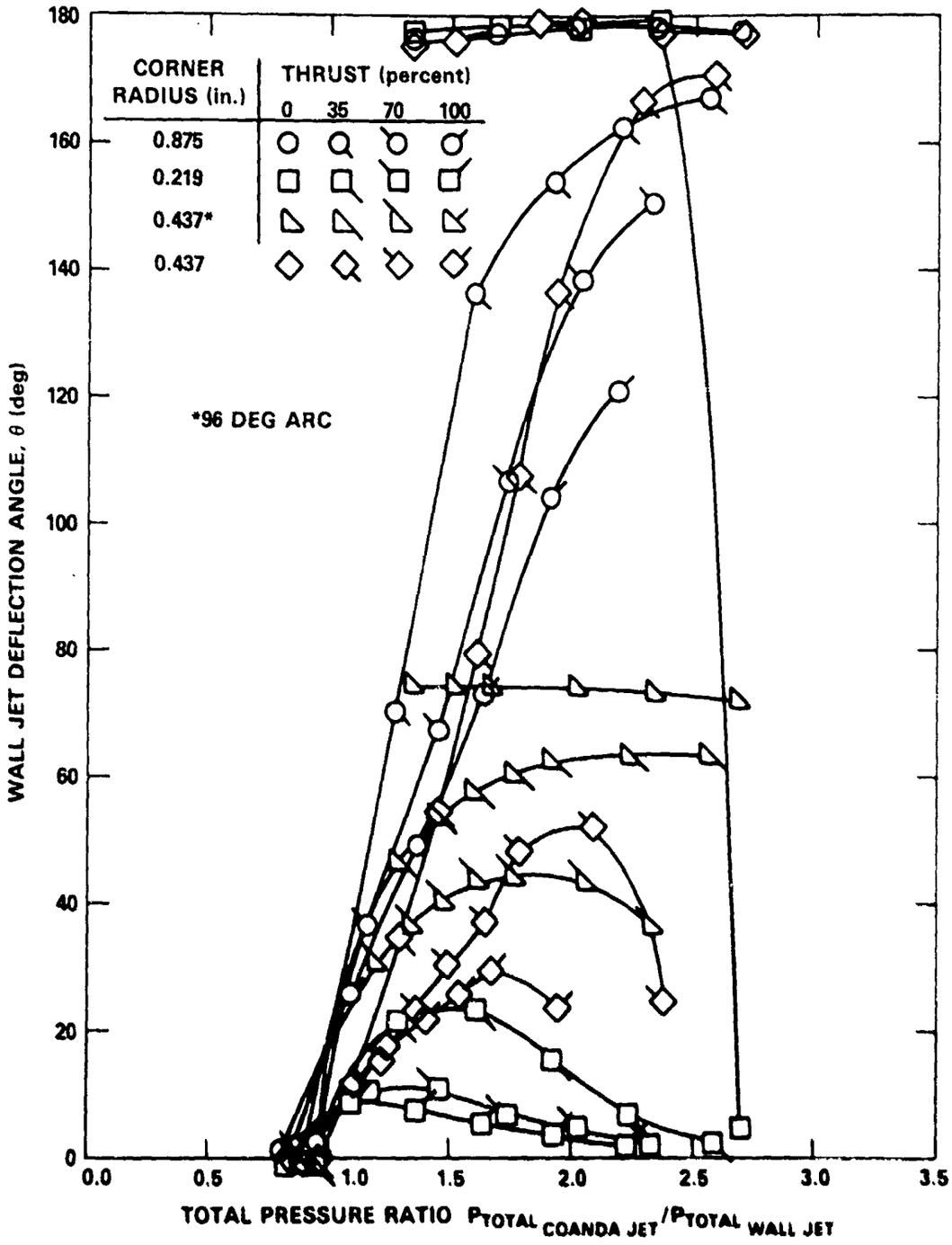

Figure 10 - $P_{T_{Coanda\ Jet}}/P_{T_{Wall\ Jet}}$ Influence on Wall Jet Deflection Performance

(Wall Jet AR = 6; Entrainment Length = 10.9 Inches; Coanda Jet Slot Height = 0.014 Inches)

Figure 11 - Wall Jet Height/Corner Radius Influence on Wall Jet Deflection Performance

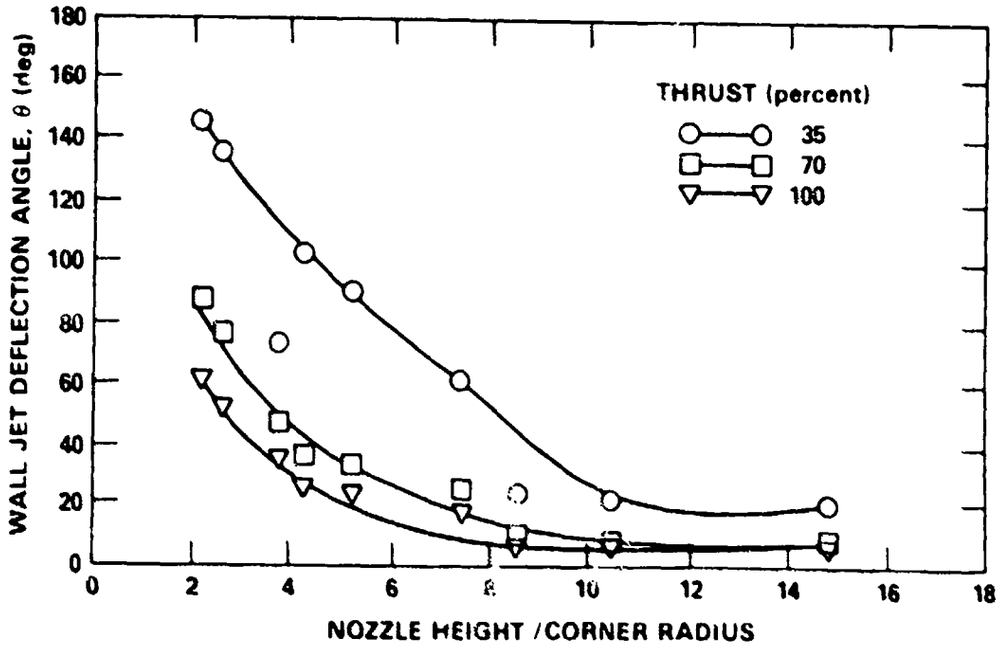

Figure 11a - Entrainment Length = 10.9 Inches; Coanda Jet Momentum = 20 Pounds; Coanda Jet Height = 0.028 Inches

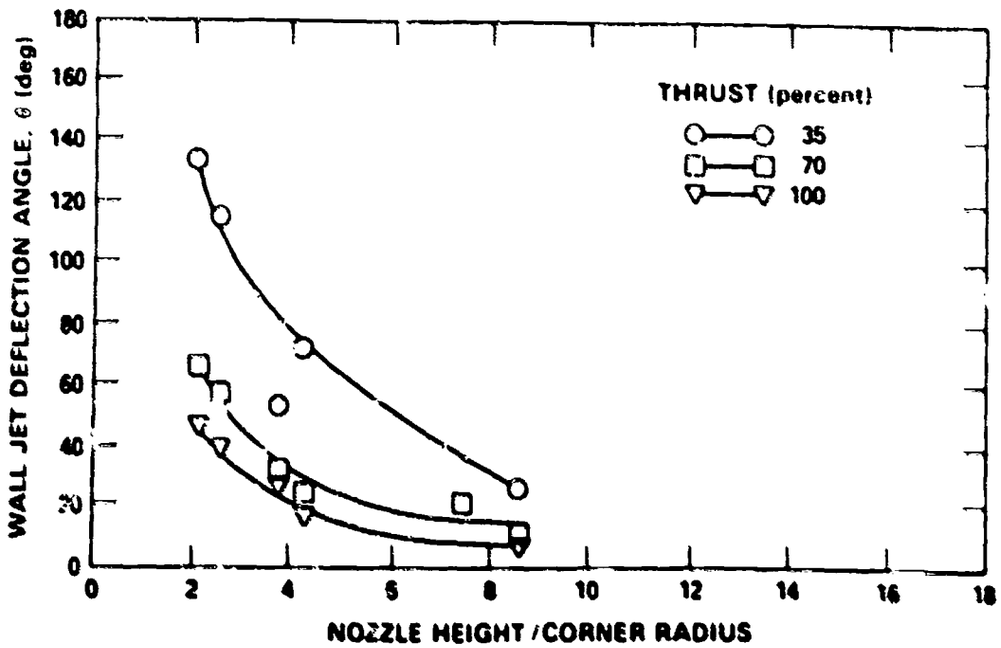

Figure 11b - Entrainment Length = 5.2 Inches; Coanda Jet Momentum = 20 Pounds; Coanda Jet Height = 0.028 Inches

Figure 11 (Continued)

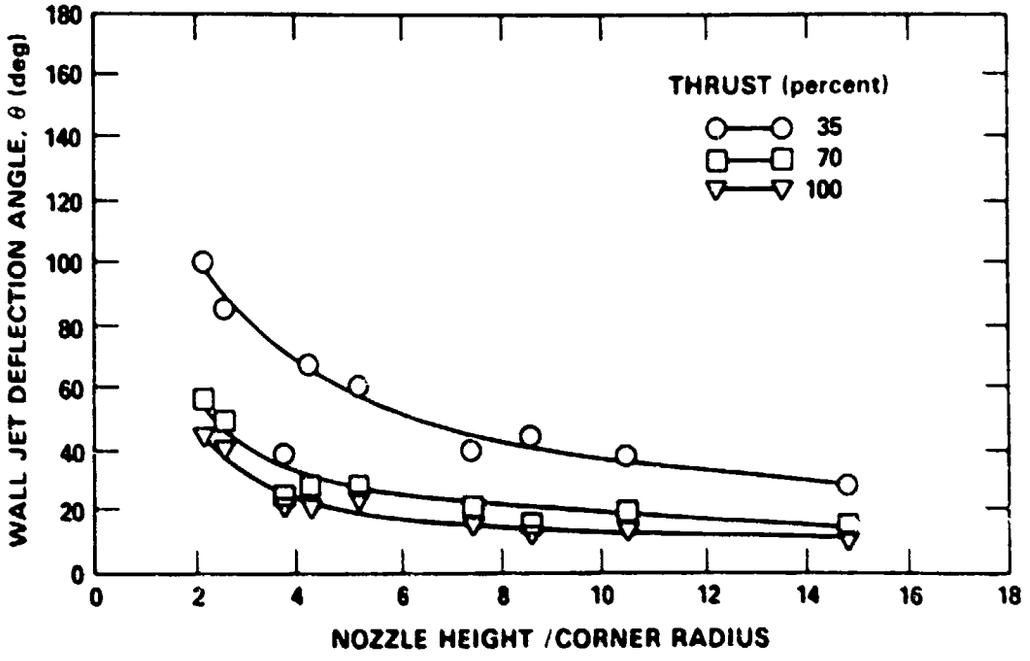

Figure 11c - Entrainment Length = 0 Inches; Coanda Jet Momentum = 20 Pounds; Coanda Jet Height = 0.028 Inches

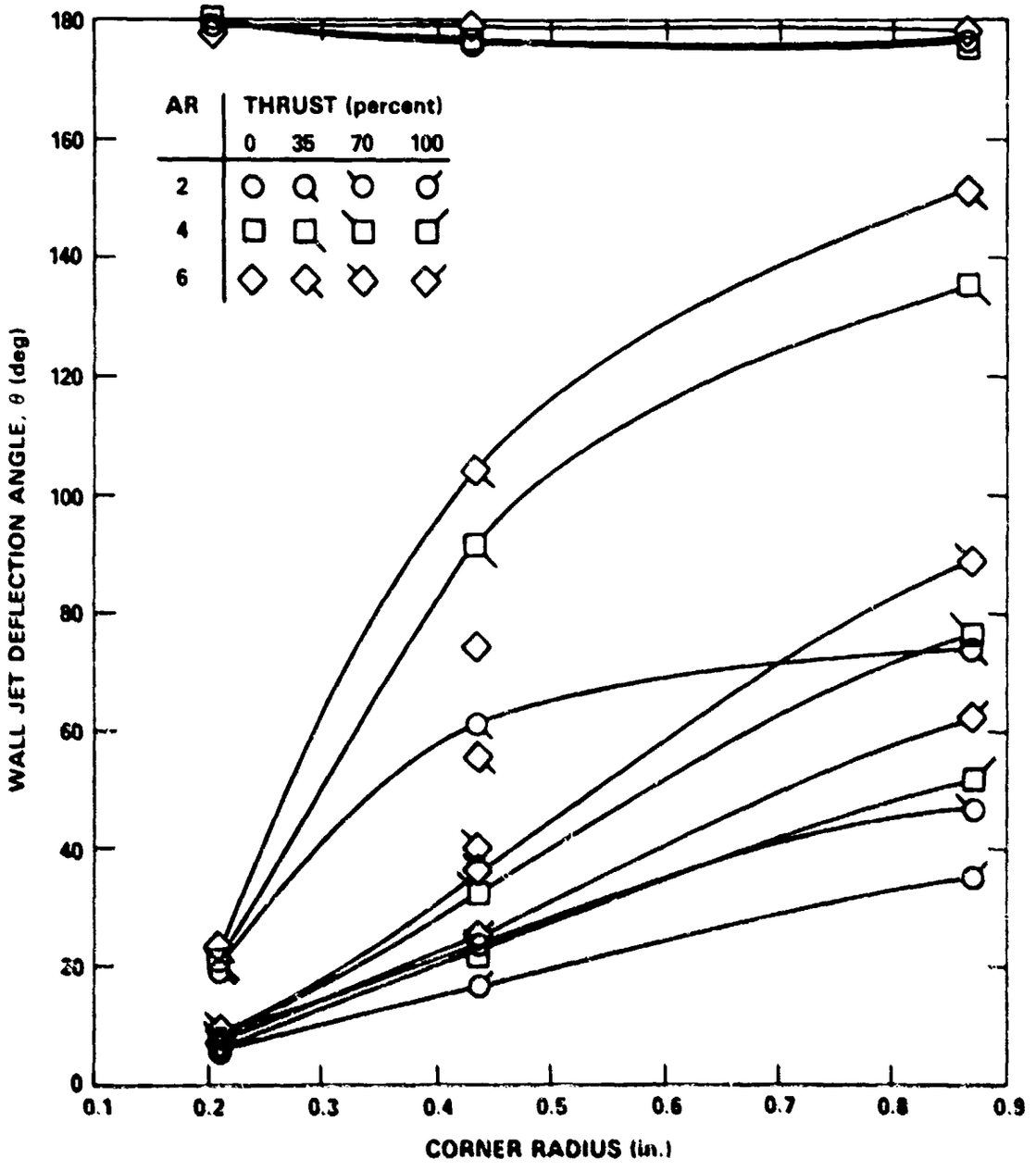

Figure 12 - Corner and Radius Wall Jet Aspect Ratio Influence on Wall Jet Deflection Performance

(Coanda Jet Momentum = 20 Pounds; Entrainment Length = 10.9 Inches; Coanda Jet Height = 0.014 Inches)

Figure 13 - Corner Radius and Entrainment Length Influence on Wall Jet Deflection Performance

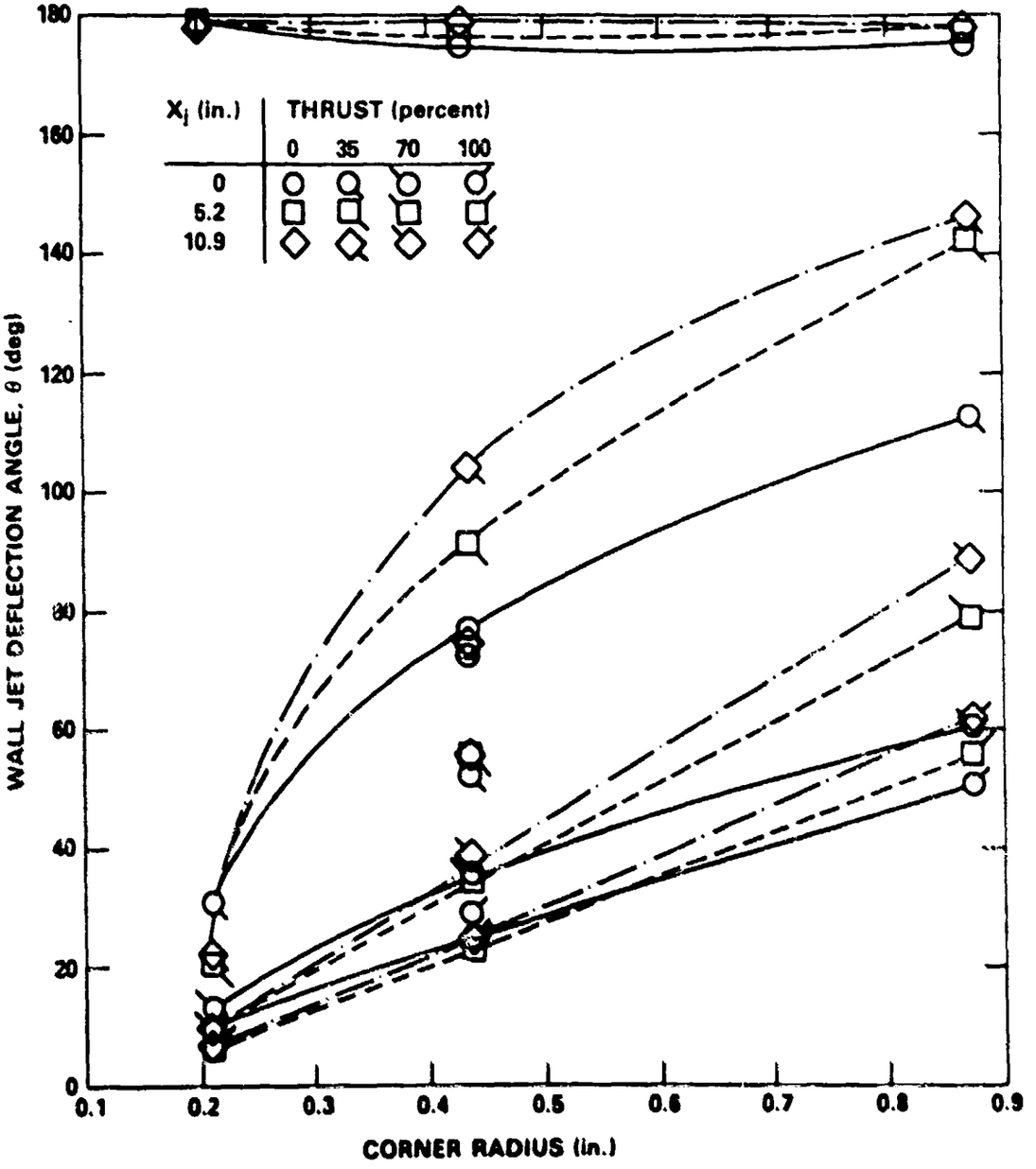

Figure 13a - Wall Jet AR = 6; Coanda Jet Momentum = 20 Pounds; Coanda Jet Height = 0.014 Inches

Figure 13 (Continued)

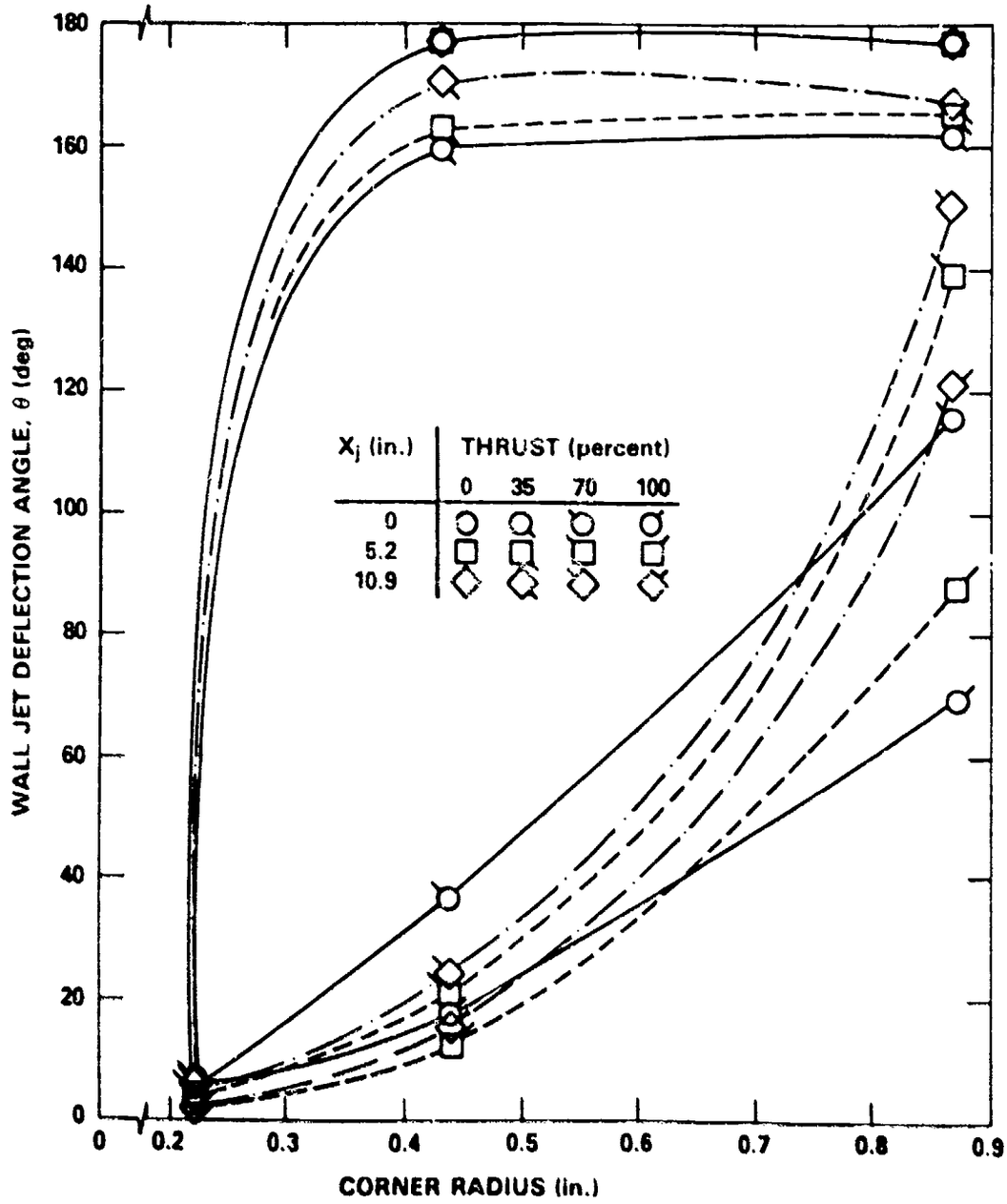

Figure 13b - Wall Jet AR = 6; Coanda Jet Momentum = 60 Pounds; Coanda Jet Height = 0.014 Inches

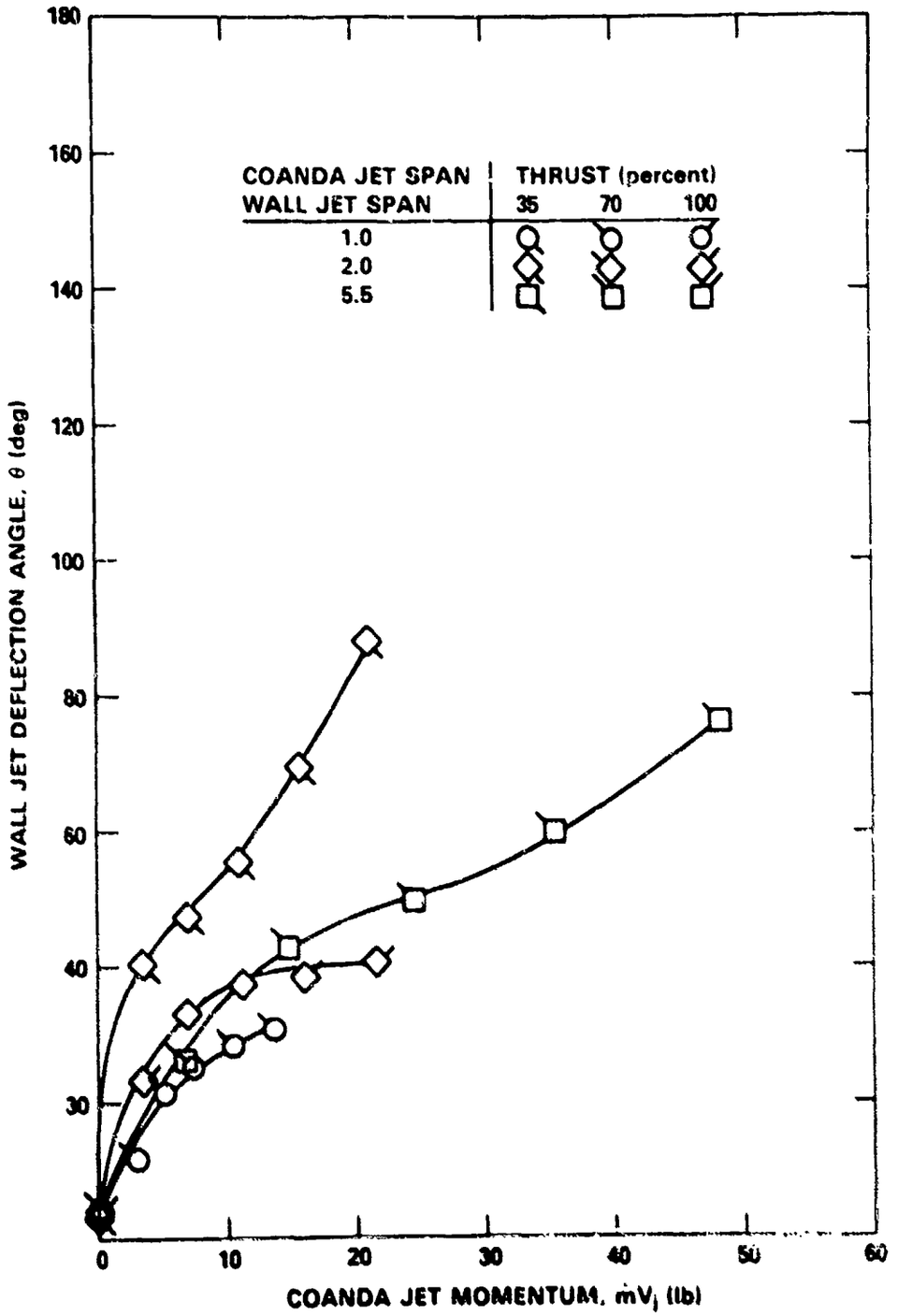

Figure 14 - Coanda Jet Span/Wall Jet Span Influence on Wall Jet Deflection Performance
(Wall Jet AR = 2; Entrainment Length = 10.9 Inches; Coanda Radius = 0.875 Inches; Coanda Jet Height = 0.014 Inches)